Studies on the Analysis of Plastic Behavior of Coal

1998

Koh Kidena

Department of Molecular Chemistry
Graduate School of Engineering
Osaka University

Studies on the Analysis of Plastic Behavior of Coal

(石炭の軟化溶融現象の解析に関する研究)

1998

Koh Kidena

Preface

The work of this thesis has been carried out under the guidance of Professor Masakatsu Nomura, the Department of Molecular Chemistry, Graduate School of Engineering, Osaka University.

The objective of this thesis is to explain the plastic phenomena of coal in view of molecular structure of coal. The detailed understanding of the plastic phenomena may be helpful to effective coal utilization for coke making. The author hopes that the results obtained in this work can contribute to further development in the area of fuel chemistry.

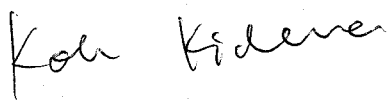

Koh Kidena

Department of Molecular Chemistry,
Graduate School of Engineering,
Osaka University
2-1 Yamada-oka, Suita,
Osaka 565-0871, JAPAN
December, 1998.

Contents

General Introduction

In Japan, over 130 million tons of coal are consumed annually[1]. Recently, the ratio of use for thermal power generation is increasing, however, even now about a half of coal consumption corresponds to the coke production for steel making. Therefore, the carbonization process is very important among coal utilization technologies. Much effort has been paid to the development of effective carbonization processes and/or replacement of the present coking process by new concept such as the direct iron ore smelting process[2] because our country has been imported almost all the coking coals and worried by a precious resource exhausting problem recently. For the development of new coking process, SCOPE 21 (Super Coke Oven for Productivity and Environment Enhancement toward the 21st Century) project has been undergoing[3]. On the other hand, the coal carbonization industry had been developing very sophisticated measurements for evaluation of coal: Gieseler fluidity and vitrinite reflectance of coal are generally used as indices for blending coals to make excellent metallurgical cokes. Gieseler fluidity seems to be a good parameter to represent thermoplastic properties of coal at high temperature, while vitrinite reflectance is considered to be a parameter related to the alignment of aromatic moieties in coal. However, these two parameters are considered to be largely based on the empirical sense and seem to lack informations about chemical reactivity of coal at a molecular level.

Under these situations, a deep understanding of plastic phenomena of coal is required. Since thermoplastic phenomena of coal actually involve various chemical reactions of its organic portion, they could be explained at the level of molecule in a scientific way. Many researchers have investigated coal plasticity so far. For example, in a review titled with *Chemistry of Coal Utilization*[4], there are systematic and detailed descriptions about plastic property of coal: investigations of the plastic property, influences of coal properties on their plastic behavior and

interpretations of the plastic property. The plastic property of coal was interpreted according to metaplast theory[5-7], where heating of coal generates metaplast, and then semicoke and gas are generated, and finally, the semicoke converts into coke and gas. Fitzgerald[5], in 1956, proposed a kinetic model of coal carbonization in plastic state. He explained the carbonization process by the metaplast theory and determined the rate constant for metaplast generation reaction. This seems to be a great contribution to understanding of plastic properties of coal at an early stage of research in this field. Besides, the γ-compound theory[8] and the importance of hydrogen transfer[9] were suggested. Snape *et al.*[10] tried to understand the phenomena of the coal plasticity by using high temperature *in-situ* ^{1}H-NMR to evaluate the mobility of coal matrix. Such technique has been applied for evaluating the rigidity of polymer. Even recently, they carbonized coal samples by using Juranek furnace and evaluated the aromatic ring size of heat-treated coal char[11]. This method is the simulation of carbonization in a coke oven. They discussed the structural differences among the coal samples experienced various temperature histories. Marzec[12] reported a new structural concept for carbonized coals where she characterized both coal and heat-treated solid products by X-ray diffraction, transmission electron microscopy and pyrolysis – field ionization mass spectroscopy, then conducted measurements of their electrical resistivities. Butterfield *et al.*[13] observed the changes of swelling and dilatation behavior during heating and discussed the coal plasticity based on the structural changes of macromolecule.

In the past two decades, the studies on chemical structure of coal were developed remarkably. Shinn[14] proposed the chemical structure model of US bituminous coal in 1984, the studies on chemical structure for coals being followed by Nomura *et al.*[15,16], Hatcher *et al.*[17] Stock *et al.*[18] and Iino *et al.*[19]. In this thesis, I would like to describe coal plasticity and coal structural change during carbonization in terms of the assembly of various kinds of chemical reactions. With referring to the investigations on coal chemical structure, the understanding concerning coal plasticity would be possible. The clarification of plasticity

phenomena is believed to lead more effective utilization of coal including coke making. One ultimate goal is the proposal of chemically rationalized parameters in place of empirical methods used in coal blending for coke making. This thesis is treating the hydrogen transfer in coal and the devolatilization behavior of coal based on metaplast theory. The results obtained in this work were shown in the following four chapters.

In chapter 1, the method for evaluating the amount of transferable hydrogen in coal was developed. The coal was heat-treated with polycyclic aromatic hydrocarbon (PAH) in a sealed tube at 420°C for 5 min. The resulting substances from the heat-treatment were recovered by CH_2Cl_2, and analyzed by GC, quantitatively. The amount of hydrogen transferred from coal to PAH was calculated from the yields of hydrogenated PAHs. This amount is extensively dependent on PAH used. It may show that different PAH was considered to abstract hydrogen atoms having different reactivity. When anthracene was used as hydrogen acceptor, the tendency of the amount of hydrogen transferred toward coal rank was similar to that of Gieseler maximum fluidity (MF). The correlation between the amount of hydrogen transferred from coal to anthracene and Gieseler fluidity of coal indicated the importance of the amount of transferable hydrogen in coal against coal plasticity.

Chapter 2 discussed what parts of coal and what kinds of reactions are concerned with the consumption of transferable hydrogen in coal described in the previous chapter. The main reaction was considered as the cleavage of bridge bonds connecting aromatic moieties. The coal samples or coal model compounds possessing bridge bonds were heat-treated in a sealed tube in the presence of hydrogen donor. 9,10-Dihydroanthracene (DHA) and 9,10-dihydrophenanthrene (DHP) were used as the hydrogen donor. From the results of heat-treatment of coal model compounds in the presence of donor, it was clear that DHP induced *ipso* position cleavage preferentially, and pointed that monomethylene linkage is important in coal structure.

Chapter 3 deals with the devolatilization behavior during thermogravimetric analysis (TGA) of coal. I found that the value of R_{max}/WL, which is the normalized maximum rate of

weight loss (R_{max}) against the total amount of weight loss (WL) was well correlated to MF of coal. R_{max}/WL value is considered to mean the effectiveness of volatilization during heating. The correlation between R_{max}/WL and MF values can be divided into two categories, C<86% and C>86%. The volatile materials are expected to act as the lubricant before devolatilization occurs. The some extent of lubricant was needed to the appearance of coal plasticity. By the FD-MS analysis of the tar fraction evolved at around temperature at T_{max}, I evaluated the molecular weight distribution and aromaticity of the fraction. This indicated the nature of low molecular weight materials evolved from coal after the state of maximum fluid.

In chapter 4, whole plastic phenomena of coal were discussed based on the results obtained in the previous three chapters and the measurement of X-ray diffraction (XRD) of coal or heat-treated coal. The XRD and SEM observation for the heat-treated coals (semicoke) showed the alignment of the aromatic lamellar structure. By referring to the results obtained by hydrogen transfer reaction, TGA and XRD, the structural change and the reaction expected to occur were explained systematically.

References

1 Institute of Energy and Resources, *Energy & Resource Handbook*, Ohmsha, Japan, 1996, p.116.

2 Annual Energy Reviews–1995, *J. Jpn. Inst. Energy* **1996**, *74*, 492.

3 Annual Energy Reviews–1994, *J. Jpn. Inst. Energy* **1995**, *73*, 601.

4 Elliot, M. A. *Chemistry of Coal Utilization Second Supplementary volume*, Wiley-Interscience, USA, 1981, Chapter 6.

5 Fitzgerald, D. *Trans. Farad. Soc.* **1956**, 362.

6 Solomon, P. R.; Best, P. E.; Yu, Z. Z.; Charpenay, S. *Energy Fuels* **1992**, *6*, 143.

7 van Krevelen, *Coal*, Elsevier, Amsterdam, 1993.

8 (a) Ouchi, K. *Fuel* **1961**, *40*, 485. (b) Ouchi, K.; Itoh, H.; Itoh, S.; Makabe, M. *Fuel* **1989**, *68*, 735.

9 Neavel, R. C. *Coal Science I*, Academic press. London, 1982, Chapter 1.

10 Maroto-Valer, M. M.; Andresen, J. M.; Snape, C. E. *Energy Fuels* **1997**, *11*, 236.

11 Maroto-Valer, M. M.; Atkinson, C. J.; Willmers, R. R.; Snape, C. E. *Energy Fuels* **1998**, *12*, 833.

12 Marzec, A. *Energy Fuels* **1997**, *11*, 837.

13 Butterfield, I. M.; Thomas, K. M. *Fuel* **1995**, *74*, 1780.

14 Shinn, J. H. *Fuel* **1984**, *63*, 1187.

15 Nomura, M.; Matsubayashi, K.; Ida, T.; Murata, S. *Fuel Process. Technol.* **1992**, *31*, 169.

16 Supplementary paper (3)

17 Hatcher, P. G.; Faulon, J.-L.; Wenzel, K. A.; Cody, G. D. *Energy Fuels* **1992**, *6*, 813.

18 Stock, L. M.; Muntean, J. V. *Energy Fuels* **1993**, *7*, 704.

19 Nakamura, K.; Takanohashi, T.; Iino, M.; Kumagai, H.; Sato, M.; Yokoyama, S.; Sanada, Y. *Energy Fuels* **1995**, *9*, 1003.

List of Publications

(1) Studies on the Chemical Structural Change during Carbonization Process

K. Kidena, S. Murata and M. Nomura

Energy Fuels, **1996**, *10*, 672-678.

(2) Quantitative Evaluation of Hydrogen Transfer Related to the Appearance of Coal Plasticity

M. Nomura, S. Murata K. Kidena and T. Chikada

Tetsu to Hagane, **1996**, *82*, 361-365.

(3) Study on Pyrolytic Behaviour of Coking Coal

M. Nomura, K. Kidena, A. Yamamoto and S. Murata

Proceedings of 8th International Conference on Coal Science, **1996**, 993-996.

(4) Consideration on Bond Cleavage Reactions of Bridge Structure in Coal Models and Coal with Two Different Hydrogen Donating Compounds

K. Kidena, N Bandoh, S. Murata and M. Nomura

Prep. Pap. of American Chemical Society, Division of Fuel Chemistry, **1997**, *42(1)*, 70-73.

(5) Investigation on Coal Plasticity: Correlation of the Plasticity and a TGA-Derived Parameter

K. Kidena, S. Murata and M. Nomura

Energy Fuels, **1998**, *12*, 782-787.

(6) Studies on the Bond Cleavage Reaction Occurred in Coal Molecule or Coal Model Compounds

K. Kidena, N. Bandoh, S. Murata and M. Nomura

J. Jpn. Inst. Energy, in contribution.

List of Supplementary Publications

(1) Solubilization of Meso-Carbon Materials by Butylation with Dibutylzinc and Butyl Iodide

Y. Zhang, K. Kidena, S. Murata, M. Nomura, Y. Yoneyama and T. Kato

Chemistry Letters, **1996**, 491-492.

(2) Solubilization of Mesocarbon Microbeads by Potassium- or Dibutylzinc-Promoted Butylation and Structural Analysis of the Butylated Products

Y. Zhang, K. Kidena, T. Muratani, S. Murata, M. Nomura, Y. Yoneyama, T. Kato and C. Yamaguchi

Energy Fuels, **1997**, *11*, 433-438.

(3) Structural Evaluation of Zao Zhuang Coal

M. Nomura, L. Artok, S. Murata, A. Yamamoto, H. Hama, H. Gao and K. Kidena

Energy Fuels, **1998**, *12*, 512-523.

(4) A Novel Orthogonal Microscope Image Analysis Method for Evaluating Solvent-Swelling Behavior of Single Coal Particles

H. Gao, L. Artok, K. Kidena, S. Murata, M. Miura and M. Nomura

Energy Fuels, **1998**, *12*, 881-890.

(6) Effects of Water and Molecular Hydrogen on Heat Treatment of Turkish Low-Rank Coals

L. Artok, H. H Schobert, M. Nomura, O. Erbatur and K. Kidena

Energy Fuels, **1998**, *12*, 1200-1211.

(5) Methyl Group Migration During Heat-treatment of Coal in the Presence of Polycyclic Aromatic Compounds

K. Kidena, N. Bandoh, M. Kouchi, S. Murata and M. Nomura

Fuel, in contribution.

Chapter 1. Transferable Hydrogen in Coal

1-1. Introduction

Based on the metaplast theory, bond cleavage reaction in coal is believed to be very important. From this viewpoint, Neavel had proposed that transferable hydrogen could stabilize radicals generated from thermal bond cleavage reaction during heat-treatment of coal[1]. Yokono and Sanada had developed the method to evaluate amounts of transferable hydrogen in coal by using reaction of coal with anthracene at 400°C[2]. Clemens *et al.* had reported that oxidation of coal led to loss of coal plasticity and addition of a solvent-soluble fraction of coal and/or polycyclic aromatic hydrocarbons to the oxidized coal resulted in restoring coal plasticity, their studies being related to the hydrogen transfer reaction in coal[3]. I am also considering that the transferable hydrogen in coal, which is consumed at the bond cleavage reactions, is important for the appearance of coal plasticity. In this chapter, the method to evaluate transferable hydrogen in coal was developed and the correlation between the transferable hydrogen and fluidity of coal was investigated. Furthermore, hydrogen sources expected in coal and their amounts were also examined.

1-2. Experimental

Samples

Eighteen coking coals were provided by the Iron and Steel Institute of Japan, Sumitomo Metal Industries Co. Ltd., and Nippon Steel Chemical Ltd., these being pulverized (-100 mesh) and dried at 100°C *in vacuo* prior to use. Proximate and ultimate analyses, and the fluidity characteristics obtained from Gieseler plastometry are summarized in Tables 1-1 and 1-2, respectively. Mainly, six coals (LS, GO, PM, WW, WB and KP) were used as the sample coals. These coals can cover the wide range of carbon content and fluidity properties. Reagents

employed were commercially available and purified by conventional recrystallization or distillation before use.

Table 1-1. Proximate and ultimate analyses of the sample coals.

Coal		Proximate analyses / wt%, db.			Ultimate analyses / wt%, daf.				
		Ash	VM	FC	C	H	N	S	O (diff.)
Luscar	LS	9.5	23.5	67.0	88.30	4.60	1.50	0.30	5.30
Goonyella	GO	9.8	23.4	66.8	88.10	5.10	1.90	0.60	4.30
Pittston-MV	PM	7.3	34.3	58.4	85.70	5.50	1.70	0.98	6.10
WarkWorth	WW	13.8	34.2	52.0	84.70	5.90	1.80	0.60	7.00
Witbank	WB	8.0	32.9	59.1	82.70	4.50	2.20	0.60	10.00
K-Prima	KP	3.8	43.4	52.8	81.20	5.90	1.30	0.40	11.20
Saraji	SJ	9.7	19.1	71.2	90.62	5.03	2.02	0.68	1.65
K-9	K9	9.4	18.2	72.4	90.03	5.18	0.92	0.23	3.64
PeakDowns	PD	10.0	20.6	69.4	89.11	5.13	1.99	0.67	3.10
Elkview	EV	9.8	20.4	69.8	88.86	5.19	1.29	0.34	4.32
Loming	LM	7.3	33.6	59.1	88.43	5.78	1.61	0.94	3.24
Quintette	QT	9.2	23.6	67.2	88.08	4.91	1.13	0.45	5.42
Eagle	EG	8.4	26.4	65.2	88.08	5.35	1.55	0.77	4.25
Black-Water	BW	9.6	26.5	63.9	87.62	5.01	2.07	0.55	4.75
Riverside	RV	9.7	22.9	67.4	86.59	5.14	1.98	0.62	5.67
K-coal	KC	7.1	34.4	58.5	84.93	5.68	1.84	0.39	7.16
PDC-HV	PH	7.7	34.0	58.3	84.10	5.63	1.64	0.94	7.69
Bank	BK	7.6	31.9	60.5	82.32	5.12	2.13	0.45	9.98

Table 1-2. Characterization of the sample coals.

Coal	Vitrinite reflectance Ro / %	Gieseler maximum fluidity log (ddpm)	Gieseler temperatues * ST ℃	MFT ℃	RT ℃
LS	1.16	2.30	420	464	490
GO	1.11	2.99	397	456	498
PM	0.93	3.81	387	438	476
WW	0.81	2.47	391	433	460
WB	0.74	0.95	412	432	446
KP	0.58	0.60	390	414	452
SJ	1.50	2.20	425	471	503
K9	1.50	1.43	450	478	505
PD	1.27	2.37	418	471	494
EV	1.26	1.65	439	471	492
LM	0.95	4.17	380	442	480
QT	1.16	2.33	420	460	487
EG	1.10	2.54	409	456	489
BW	1.04	1.78	408	447	473
RV	1.10	2.78	410	450	485
KC	0.76	2.20	396	434	464
PH	0.81	3.89	391	438	468
BK	0.74	0.78	407	424	447

* ST = Softening temperature, MFT = Maximum fluidity temperature, RT = Resolidification temperature

The reaction of coal with PAHs

A sealed tube (Pyrex, 6 mm inner diameter x 100 mm long) containing a 1:1 mixture (weight ratio, totally 100 or 200 mg) of coal and polycyclic aromatic hydrocarbon (PAH) was placed in an electric furnace preheated at 420°C, then being kept for 5 min. The temperature inside the sealed tube raised up to a desired temperature within 2 min, the heating rate becoming about 200 K/min. After 5 min passed, the sealed tube was taken out, then products inside the tube being recovered with dichloromethane. Qualitative and quantitative analyses of the products were undertaken by a Shimadzu QP-2000A GC/MS and a Shimadzu GC-14APFSC gas chromatograph with CBP-1 column (0.25 mm diameter x 25 m long), respectively.

Semiempirical MO calculations

All MO calculations were carried out on an Apple Macintosh computer by using a semiempirical molecular orbital calculation program, CAChe (Computer Aided Chemistry) MOPAC 94, which was purchased from CAChe Scientific Inc. The values of heat of formation for the PAHs and their hydrogenated ones were determined by solving the Schrödinger equation using the AM1 semiempirical Hamiltonian. The difference of the standard heat of formation [$\Delta(\Delta H_f)$] was calculated as follows: $\Delta(\Delta H_f) = \Delta H_f$ (di-hydrogenated compound) – ΔH_f (aromatic compound), where ΔH_f is a standard heat of formation of each compound.

Solid state SPE/MAS ^{13}C-NMR measurements

Solid state SPE/MAS ^{13}C-NMR spectra were recorded on a Chemagnetics CMX-300 spectrometer with MAS method (10-10.5 kHz). For the measurements, about 100-150 mg of coal was packed into a zirconia sleeve (ϕ 5 mm x 8 mm long). The measurement parameters were as follows: 200 or 100 sec pulse delay, 45° pulse width, and over 400 scans. Deconvolution of the spectra was conducted on an Apple Macintosh computer with a commercial NMR data

processing software, MacAlice (Ver. 2.0, JEOL DATUM). The resulting spectra were divided into twelve Gaussian curves. According to the chemical shifts of model compounds reported by Hayamizu *et al.*[4], these could be assigned as following eleven types which are believed to be present in coal: carbonyl (C=O: peak top, around 187 ppm), aromatic carbon connected to oxygen (Ar-O: 167 and 153 ppm), aromatic carbon connected to other carbon (Ar-C: 140 ppm), aromatic bridgehead and/or aromatic tertiary carbon (Ar-C,H: 126 ppm; Ar-H: 113 ppm), aliphatic carbon connected to oxygen (-OCH_2O-: 93 ppm; -O-CH_2-, -OCH_3: 56 ppm), aliphatic carbon of bridge methylene type (CH_2': 40 ppm), aliphatic carbon of methylene type in alkyl chain (CH_2: 31 ppm), methyl group at α-position to aromatic ring (α-CH_3: 20 ppm), and methyl group at terminal position of alkyl chain (*t*-CH_3: 13 ppm). Each deconvoluted curve has an appropriate width to fit to original spectrum.

Measurement of diffuse reflectance FT-IR

Diffuse reflectance FT-IR spectra were recorded on a Shimadzu FTIR-8100M spectrometer equipped with DRS-8000 unit. The coal sample (30 mg) was mixed with pure KBr (270 mg) by using a mechanical grounder. Scan number of 1024 was applied for each measurement and obtained data were treated with Kubelka-Munk conversion which is conventional method to get quantitative data from diffuse reflectance FT-IR spectra.

1-3. Results and Discussion

1-3-1. The reaction of coal with various PAHs

In order to observe the amount of transferable hydrogen in coal, the reactions of coal with several hydrogen acceptable PAHs such as anthracene (ANT), naphthacene (NAC), acridine (ACR) and pyrene (PYR) were conducted at 420°C for 5 min in a sealed tube. Under these conditions, the additive reagents are expected to act as hydrogen acceptor. For example, the

reaction of coal with ANT gave 9,10-dihydroanthracene (DHA) and 1,2,3,4-tetrahydro-anthrancene (THA) as major hydrogenated products accompanied by minor amounts of methylanthracenes (MA). A recovery of anthracene derivatives (sum of yields of ANT, DHA, THA and MA) was enough high (>90%) to discuss hydrogen transfer reaction between coal and ANT. Heat-treatment of ANT without coal was also carried out, this affording no detectable amount of hydrogenated products along with the quantitative recovery of ANT. These results indicated that neither disproportionation nor polymerization of ANT occurs in this system. The amount of hydrogen transferred from coal to PAH was estimated according to the following equation:

The amount of hydrogen transferred (mg-H_2/g-daf coal)

= (wt of THA x 4/182 + wt of DHA x 2/180) x 1000/wt of daf coal

The plots of the amount of hydrogen transferred against carbon content of coal were shown in Figure 1-1. In this case, six coals were used as the sample coals. Depending on the kinds of PAHs, amount of hydrogen transferred changed drastically. In the reaction of coals with PYR,

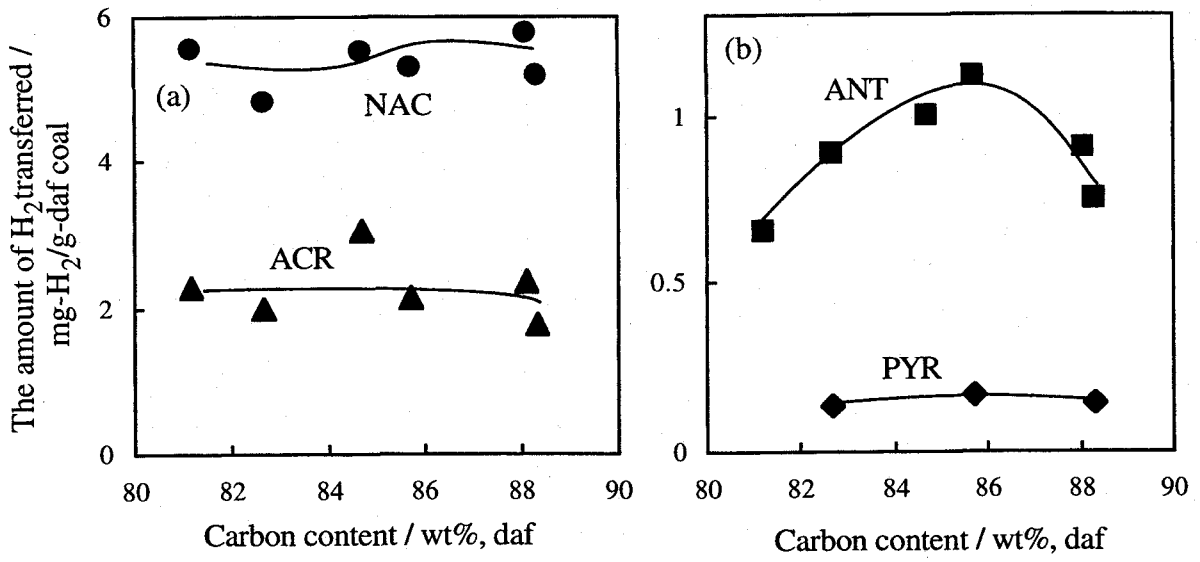

Figure 1-1. Relationships between carbon content and the amount of hydrogen transferred from the coals to (a) NAC, ACR and (b) ANT, PYR.

the amount of hydrogen transferred was rather small (<0.15 mg-H_2/g-coal), this suggesting that PYR could hardly abstract hydrogen from these coals (Figure 1-1b). On the other hand, about 5 mg of hydrogen in 1 g of coals was transferred from coals to NAC, in case of ACR, 2-3 mg of hydrogen was transferred (Figure 1-1a). The results of the reaction of coal with ANT showed interesting tendency: the amount of hydrogen transferred from coal to ANT increased with increase of carbon contents of the coal and then turned to decrease with a maximum value at PM coal (Figure 1-1b). Furthermore, in the case using 9-methylanthracene (9MA) as hydrogen acceptor, ANT was produced (in 2-10 wt% yield) along with the normal hydrogenated compounds like 9,10-dihydro-9-methylanthracene (DHMA). These results might suggest that transferable hydrogen in coal molecule played a role for not only stabilization of the radicals generated by bond fission, but also acceleration of aryl-alkyl bond cleavage by *ipso*-hydrogen attack as indicated next chapter.

The reactivity of these PAHs toward coal could be rationalized on the basis of the results of semiempirical molecular orbital calculation. The experimental or calculated values of heat of formation for a series of PAHs and hydroaromatics have not been reported, so I conducted the semiempirical molecular orbital (MO) calculations. Table 1-3 summarizes the standard heat of

Table 1-3. The difference of heat of formation calculated by MOPAC-AM1 method.[a]

PAH		$\Delta H_f(A)$[b] kcal/mol	$\Delta H_f(H_2A)$[b] kcal/mol	$\Delta(\Delta H_f)$[c] kcal/mol
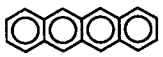	NAC	86.9	57.7	– 29.2
	ACR	77.2	49.7	– 27.5
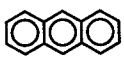	ANT	62.9	38.3	– 24.6
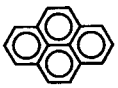	PYR	67.4	49.4	– 18.0

[a] Applied multiplicity was singlet for aromatic and di-hydrogenated aromatic compounds.

[b] A : Aromatic compound, H_2A : Di-hydrogenated aromatic compound

[c] $\Delta H_f(H_2A) - \Delta H_f(A)$.

formation of these PAHs and their dihydrogenated ones by MO calculation program, MOPAC-AM1. Difference of these values ($\Delta(\Delta H_f)$) obeyed the following sequences: NAC (29.2 kcal/mol) ACR (27.5) > ANT (24.6) > PYR (17.9). This order agrees well with the amount of hydrogen transferred from coal to the acceptors. Here, assuming the difference of heat of formation between reactive site of coal molecule toward dehydrogenation reaction and its dehydrogenated form as $\Delta(\Delta H_c) = \Delta H_f(\text{coal}) - \Delta H_f(\text{coal-H})$, overall heat of the reaction will be $[\Delta(\Delta H_c) + \Delta(\Delta H_f)]$. Therefore, NAC thought to abstract the hydrogen from the sites with lower reactivity, *i.e.*, larger $\Delta(\Delta H_c)$.

1-3-2. Evaluation of the amount of methylene carbons from ^{13}C-NMR measurement

The results of hydrogen transfer reaction indicated that coal has several kinds of hydrogen atoms transferring to hydrogen acceptors. The candidate for specific hydrogens may be the one located at naphthenic rings such as the center ring of 9,10-dihydroanthracene and aliphatic substituents linked with aromatic rings such as the methylene position of diarylmethane or 1,2-diarylethane. Clemens *et al.* had pointed out that ethylene bridges between two aromatic moieties (e.g. 1,2-diphenyl-ethane) and hydroaromatic sites played an important role in coal plastic stage[3c]. Therefore, I tried to evaluate the amounts of these kinds of functional groups in coal on the basis of the data from ^{13}C-NMR measurements.

Table 1-4. Chemical shifts of several methylene carbons.

	Chemical shift (ppm)
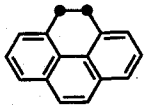	28.64
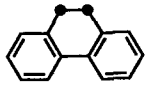	28.94
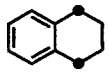	29.41
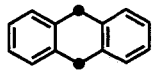	36.02
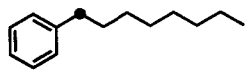	36.08
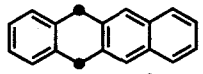	36.83
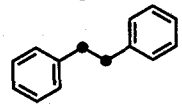	37.88
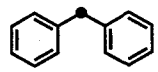	41.91

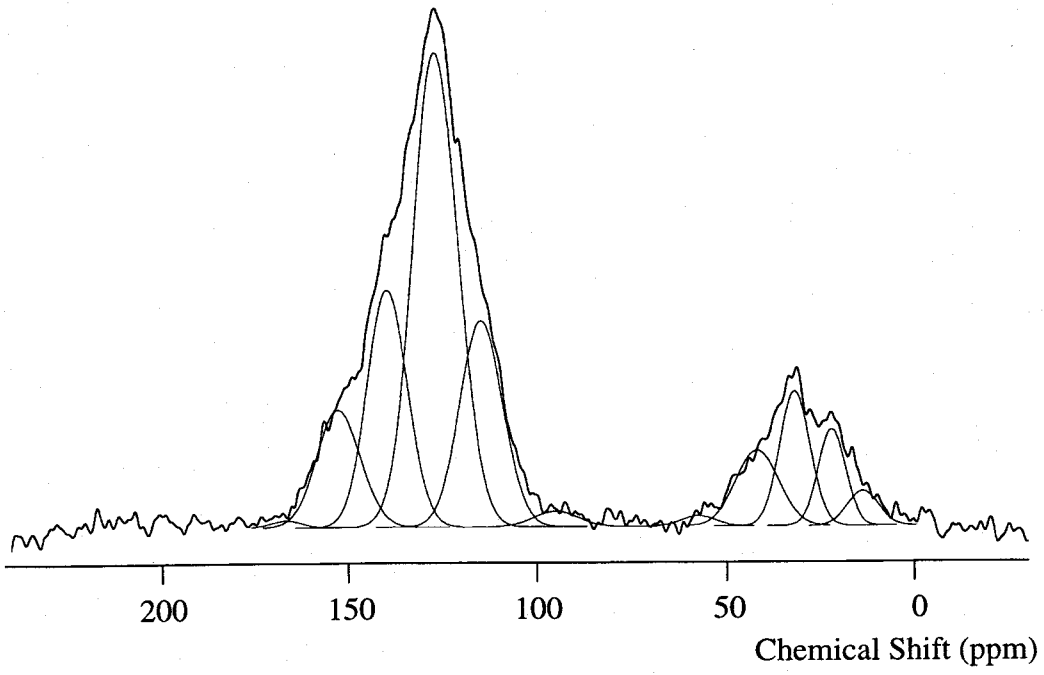

Figure 1-2. Solid state ^{13}C-NMR spectrum of coal and deconvoluted curves.

An example of ^{13}C-NMR spectrum and the deconvoluted curves of a sample coal was shown in Figure 1-2. Aliphatic region (<70 ppm) of the spectra was separated into 5 kinds of carbon such as terminal methyl (peak top, around 13 ppm), α-methyl to the aromatic moieties (20 ppm), methylene (31 and 40 ppm), and methyl or methylene attached to the oxygen functional group (56 ppm). The assignments of methylene carbons are given from the several coal model compounds[4] as shown in Table 1-4. The methylene carbons in dihydroarenes such as 9,10-dihydroanthracene or 9,10-dihydrophenanthrene can release hydrogen easily, but these carbons can't be separated from other types of carbons by the chemical shift in detail. Here, whole amount of methylene carbons was considered. The carbon distribution was evaluated from the peak intensity of the deconvoluted curves. The area intensity of each curve gave the amount of each type of carbon. Methylene carbon (31 and 40 ppm) was 5.6 – 15.2% (Table 1-5), so the amounts of hydrogen on methylene carbon were calculated as 0.46 – 1.27% (5.6/12 – 15.2/12) because one methylene carbon has one transferable hydrogen atom. Comparing these values with the amount of hydrogen transferred from coal to ANT (0.06 – 0.11%), these values were rather

large. However, the amount of hydrogen on methylene carbon estimated by ^{13}C-NMR contains hydrogen on less reactivity such as methylene carbons in alkyl side chains. Therefore, the amount of hydrogen transferred from coal to NAC (5 mg-H_2/g-daf coal = 0.5%) seemed to be too large, and NAC can abstract hydrogen atoms from less reactive sites. For the evaluation of active (means release hydrogen easily) methylene carbon, simplification of the assignment was tried. Although some kinds of active methylene carbons such as methylene group in 9,10-dihyrophenanthrene (Table 1-4), α-methylene carbon to aromatic ring tends to appear in lower magnetic field (40 ppm) than other methylene carbon. By subtracting the amount of terminal methyl (13 ppm) which corresponds to that of α-methylene carbons in long alkyl side chains from that of α-methylene carbon (40 ppm), the amount of hydrogen on active methylene carbon was estimated as 0.17 – 0.25%. These values were similar to the amount of hydrogen transferred from coal to ANT. Consequently, I thought that only a part of aliphatic hydrogen which had an appropriate activity seemed to be effective for development of coal plasticity.

Table 1-5. The amount of CH_2 evaluated from ^{13}C-NMR and elemental analysis data.

Coal	wt% of carbon assigned as CH_2 [a]	wt% of hydrogen on CH_2 group [b]
Luscar	5.6	0.46
Goonyella	7.4	0.62
Pittston-MV	12.9	1.08
WarkWorth	12.5	1.04
Witbank	11.7	0.97
K-Prima	15.2	1.27

* each value was based on weight of coal.
[a] CH_2 (%, carbon distribution) obtained from NMR data x C% (elemental analysis)
[b] wt% of C as CH_2 / 12

1-3-3. The correlation between the amount of transferable hydrogen in coal and Gieseler fluidity

The plot of the amount of hydrogen transferred from coal to ANT against carbon content of coal showed a distinctive tendency. Therefore, the reactions of 12 kinds of coals other than 6

coals mentioned already with ANT were conducted and evaluated the transferable hydrogen in coal. The data were shown in Figure 1-3. The amount of hydrogen transferred from coal to ANT increased with increase of carbon contents of coal and then turned to decrease with a maximum value at around C 86%.

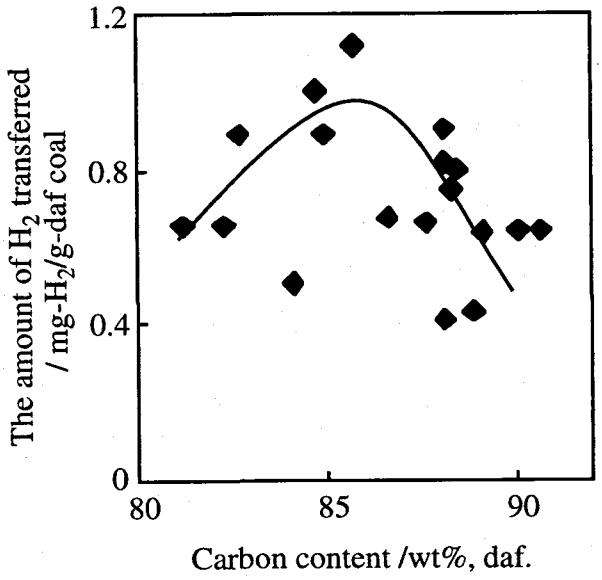

Figure 1-3. Plot of the amount of hydrogen transferred from coal to anthracene against carbon content of coal.

The tendency of this curve was similar to the plot of Gieseler fluidity of coal against carbon content of coal as shown in Figure 1-4. Therefore, the correlation between the amount of hydrogen transferred from coal to ANT and Gieseler fluidity was examined. The plot between them is shown in Figure 1-5. These two parameters somewhat correlated each other, so it was suggested that the specific transferable hydrogen in coal plays a very important role in the plastic stage of coal as mentioned by Neavel[1] and Clemens[3c,3d]. This fact implied that the other factors than the amount of transferable hydrogen affected to the appearance of coal plasticity. However, when the data plotted were checked in detail, it was

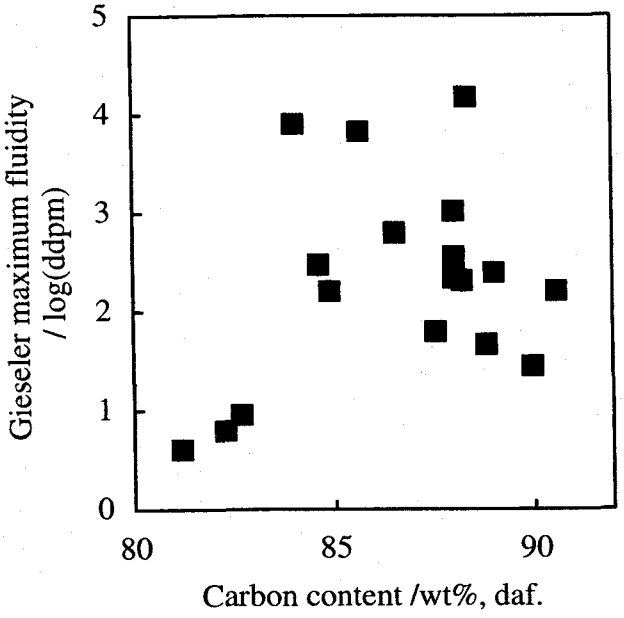

Figure 1-4. Plot of the Gieseler maximum fluidity of coal against carbon content of coal.

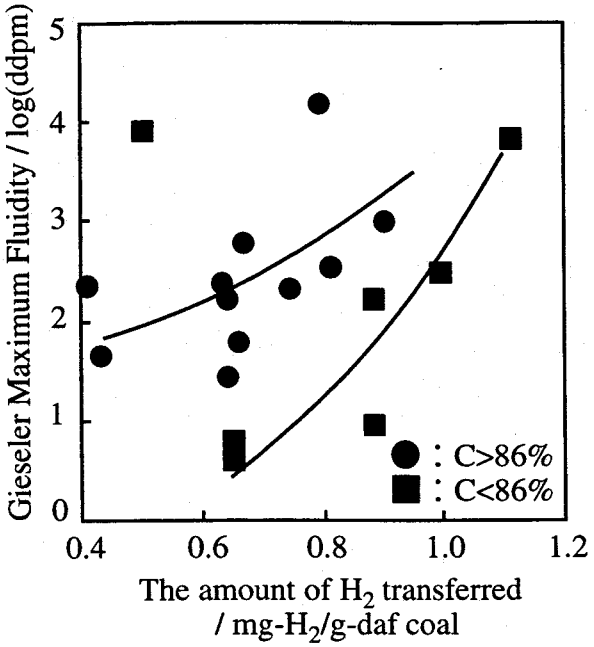

Figure 1-5. Correlation between Gieseler maximum fluidity and the amount of hydrogen transferred from coal to anthracene.

revealed that the tendency could be divided into two groups; C (carbon content of coal) >86% and C<86%. Higher rank coals show higher fluidity even with the small amount of transferable hydrogen, *vise versa*, large amount of transferable hydrogen was needed to show the plasticity of lower rank coals. The amount of hydrogen consumption in the reaction of coal with hydrogen donor was larger in lower rank coal as mentioned in chapter 2.

1-3-4. Source of transferable hydrogen in coal

The possible source of transferable hydrogen was considered as the methylene carbon in hydroaromatic structure such as 9-position carbon in 9,10-dihydroanthracene. In order to investigate the structural change during heat-treatment of coal with PAH, the reaction residue was analyzed by solid state ^{13}C-NMR and diffuse reflectance FT-IR. For these measurements, the CH_2Cl_2 insoluble fraction from the reaction of coal with PAH was collected.

Analysis of the residue after hydrogen transfer reaction by ^{13}C-NMR and diffuse reflectance FT-IR spectroscopy

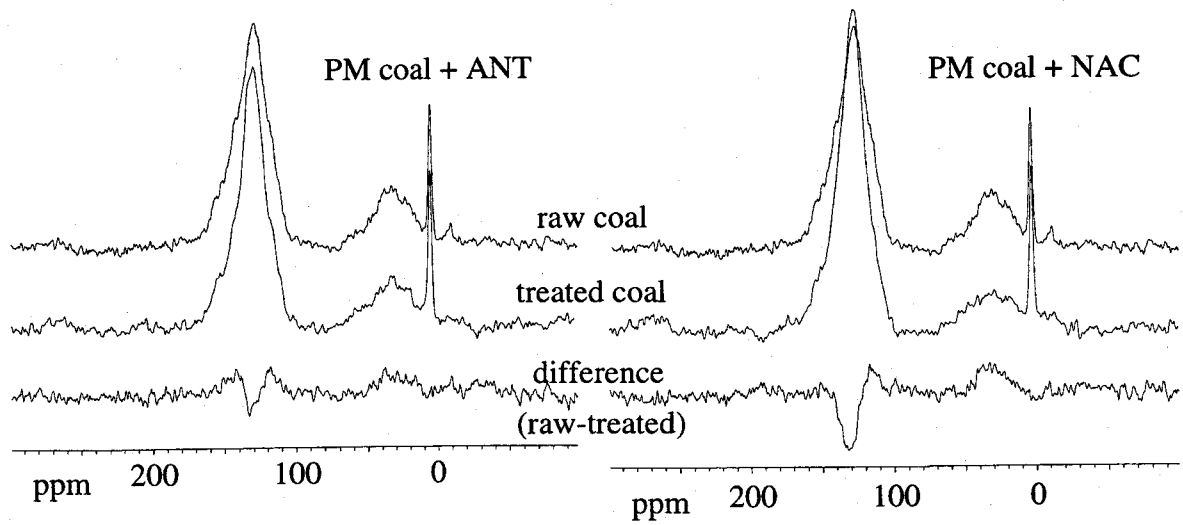

Figure 1-6. ^{13}C-NMR spectra of raw and heat-treated (with ANT or NAC) Pittston-MV coals and their difference spectra.

In order to quantify the carbon species, tetrakis(trimethylsilyl)silane (TKS) was added to the residue in a determined ratio (TKS:coal = 1:10, w/w) as an internal standard. This compound does not react with coal molecule. The spectra for Pittston-MV (PM, 85.7% C) coal and the treated PM coals are shown in Figure 1-6, the difference spectra also being cited. In these difference spectra, upward peak corresponded decrease of carbon by the reaction with ANT or NAC. The spectra showed that aliphatic portion of carbon was decreased whereas aromatic carbon was increased. Quantitatively, the residue treated by NAC showed larger change in both regions of aliphatic and aromatic parts. This agreed with the amount of transferred hydrogen from coal to PAHs. NAC abstracted more amount of hydrogen from coal. Then, the data analyses were conducted from the evaluation of the carbon distribution of coal and the treated coals by curve-fitting method. The data are summarized in Table 1-6. They showed that relative change between 30 ppm and 40 ppm, slightly larger change in 40 ppm around can be seen with the ANT treated sample. Peak at 40 ppm corresponds to methylene carbons in hydroaromatic compounds such as 9,10-dihydroanthracene (36 ppm). Therefore, it can be thought that NAC is probably to subtract hydrogen from not only hydroaromatic moieties but also methylene carbons which is difficult to release hydrogen.

Table 1-6. ^{13}C-NMR data for raw, anthracene treated and naphthacene treated (420°C, 5 min) Pittston-MV coals.

sample	area ratio to TKS		
	CH_2' (40 ppm)	CH_2 (30 ppm)	Ar-H, Bridgehead (113, 126 ppm)
raw	1.23	1.25	9.26
anthracene-treated	1.09	1.12	11.05
naphthacene-treated	0.85	0.63	11.41

TKS=tetrakis(trimethylsilyl)silane
Chemical shift values represent the center of the peak in curve-fitting treatment of the spectra.

Decreases in CH_2 and increases in aromatic C-H were also supported from the FT-IR data as shown in Figure 1-7. From this figure, peak intensity ratios, C-H(CH_2) (appeared at 2926 cm^{-1}) / C_{Ar}-H (3040 cm^{-1}) were calculated as 3.9, 2.8, 2.2 and 1.4 for raw, pyrene-treated, anthracene-treated and naphthacene-treated Pittston-MV coals, respectively.

Both analyses of the reaction residue indicated the increase of aromatic C-H and the decrease of CH_2. The plausible structural change corresponding to the data was dehydrogenation

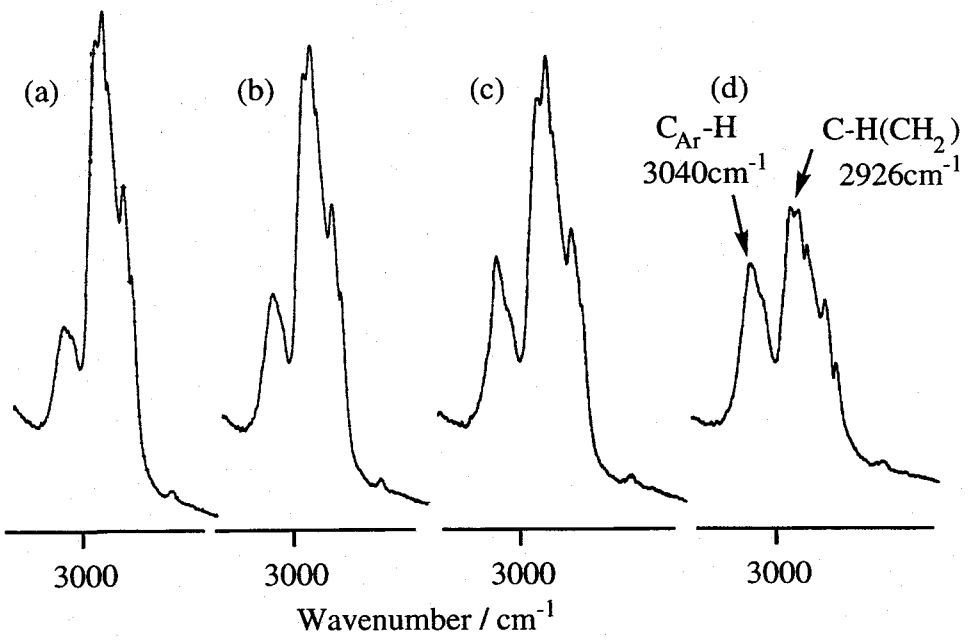

Figure 1-7. Diffuse reflectance FT-IR spectra of (a) raw, (b) pyrene-treated, (c) anthracene-treated and (d) naphthacene-treated (420°C, 5min) Pittston-MV coal.

from hydroaromatic sites. Therefore, probable hydrogen source during the reaction of coal with ANT was the methylene carbons contained in hydroaromatic parts.

The reaction of model compounds possessing plausible hydrogen donor site with PAHs.

Most plausible hydrogen source was considered as hydroaromatic structure of coal. This was also supported by the reaction of coal model compounds with PAHs. 9,10-Dihydrophenanthrene, 1,2-diphenylethane and 9-butylanthracene were selected as the model possessing methylene carbon in hydroaromatic, methylene bridge and methylene group in side chain, respectively. These compounds were treated with NAC, ANT or PYR in a sealed tube at 420°C for 5 min. The conversion of PAH to hydrogenated PAH is shown in Table 1-7. Hydrogen in methylene carbon of hydroaromatic portion could transfer to each PAH, but the amount transferred to PAH was the order of NAC > ANT > PYR. This was consistent with the results obtained from the reaction of coal with PAHs. In comparison among the three model compounds having various methylene groups, hydroaromatic structure could release hydrogen most easily whereas methylene carbons in side chain didn't give any hydrogen. However, NAC abstracted small amount of hydrogen even from side chain.

Table 1-7. The results of the reaction of model compouds with plausible hydrogen source and PAHs.

Model compounds		Conversion of PAH / mol%		
		NAC	ANT	PYR
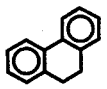	Methylene in hydroaromatic	70	15	0.7
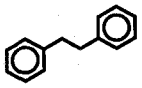	Methylene bridge	9	trace	0
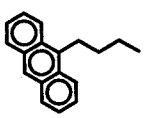	Methylene in side chain	trace	0	0

reaction conditions: [PAH]:[model compound] = 100mg:100mg, in a sealed tube, 420°C, 5min.
conversion of PAH to hydrogenated PAH was determined by GC analysis.

The results obtained here supported that most plausible source of transferable hydrogen was the hydroaromatic sites in coal. Furthermore, the sequence of the hydrogen acceptability of PAHs could be also explained. NAC had high hydrogen acceptability and could abstract hydrogen atom from methylene carbons in side chain.

1-4. References

1 R. C. Neavel, *Coal Science I*, Chapter 1, Academic Press, London, 1982.

2 (a) Yokono, T.; Marsh, H.; M. Yokono *Fuel* **1981**, *60*, 607. (b) Yokono, T.; Obara, T.; Iyama, S.; Yamada, J.; Sanada, Y. *Nenryo Kyokaishi* **1984**, *63*, 239. (c) Yokono, T.; Takahashi, N.; Sanada, Y. *Energy Fuels* **1987**, *1*, 360.

3 (a) Clemens, A. H.; Matheson, T. W. *Fuel* **1987**, *66*, 1009. (b) Clemens, A. H.; Matheson, T. W.; Sakurovs, R. *Fuel* **1989**, *68*, 1162. (c) Clemens, A. H.; Matheson, T. W. *Fuel* **1992**, *71*, 193. (d) Clemens, A. H.; Matheson, T. W. *Fuel* **1995**, *74*, 57.

4 Yamamoto, O.; Hayamizu, K.; Yanagisawa, M.; Yabe, A.; Sugimoto, Y. *J. Jpn. Inst. Energy* **1994**, *73*, 267.

Chapter 2. Analysis of Hydrogen Transfer Reaction Occurred in the Heat-treatment of Coal

2-1. Introduction

Coal organic materials (COM) is believed to be an amorphous polymer consisting of aromatic clusters with aliphatic side chains or bridges including naphthenic portion. Accordingly, COM should be described by certain chemical formula as other synthetic or natural polymers are. Using various analytical tools, coal chemical structure had been investigated at a level of molecule, however, COM is essentially far from the synthetic polymer. It does not contain any repeated units but many kinds of moieties and shows different behavior in its conversion reaction depending on its rank or its mining region. From these complexities, information concerning the chemical structure and the reactivity of coal is now still limited.

In coal utilization processes such as liquefaction, gasification or carbonization, decomposition of COM should be important. In chapter 1, I mentioned the importance of the transferable hydrogen in coal, these transferable hydrogens being thought to be consumed to decomposition of COM. There are many investigations which applied the coal models having the bridge structures as contained in coal and pursued the fashion of the reaction using the model compounds. Autrey *et al.*[1], Futamura *et al.*[2] and Nomura *et al.*[3] had mentioned the pyrolysis or hydrogenolysis of diarylmethane, while Korobkov *et al.*[4] reported the rate constants of thermolysis of diaryl or alkylethers in detail and discussed about their mechanisms. As to the thermal behavior of side chains, Savage *et al.*[5] examined 1-alkylpyrene pyrolysis, and Nomura *et al.*[6] and Freund *et al.*[7] picked up the aromatic compounds having longer bridges or alkyl side chains. As to the mechanisms of the bond cleavage reactions occurred in coal, McMillen *et al.* proposed radical hydrogen transfer (RHT), which was also discussed by other researchers[1,8,9].

In this chapter, in order to investigate the significant reaction site and reaction pathway,

the heat-treatment of coal or coal model compounds with hydrogen donor was performed. The results obtained from the heat-treatment of coal or coal model compounds were compared each other to discuss the bond cleavage reaction occurred in coal molecules.

2-2. Experimental

Samples

Coal samples employed in this chapter are the 17 kinds of coals. 11 of them were the coal samples shown in Tables 1-1 and 1-2 (LS, GO, PM, WW, WB, KP, SJ, EG, BW, LM and KC), other 6 coals were the subbituminous and bituminous coals, their proximate and ultimate analyses were shown in Table 2-1. Coal samples were pulverized (–100 mesh) and dried at 100°C for 6 h *in vacuo* prior to use. The model compounds, 1,2-di(1-naphthyl)ethane (DNE) and 1,5-dibenzylnaphthalene (DBN), were synthesized as follows: DNE was prepared by reduction of 1-(chloromethyl)naphthalene with iron powder in water [10] and DBN was obtained by Et_3SiH/CF_3COOH reduction of 1,5-dibenzoylnaphthalene according to the method reported elsewhere[11]. The other reagents or coal model compounds such as 1,2-diphenylethane (DPE) and benzylphenylether (BPE) were commercially available and purified by conventional recrystallization before use.

Table 2-1. Proximate and ultimate analyses of the sample coals.

		Proximate anal. / wt%, db.			Ultimate anal. / wt%, daf.				
Coal	code	Ash	VM	FC	C	H	N	S	O(diff.)
Newlands	NL	15.36	26.98	57.66	85.90	4.87	1.70	0.48	7.04
Ebenezer	EB	14.85	38.90	46.22	81.19	6.06	1.57	0.58	10.60
Blair Athol	BA	8.82	29.32	61.86	82.92	4.72	1.83	0.31	10.23
Tatung	TT	10.00	29.70	60.31	82.66	4.68	1.06	0.73	10.87
Taiheiyo	TH	12.55	45.70	41.75	78.72	6.22	1.17	0.11	13.78
Tiger Head	TG	12.17	36.30	51.54	82.25	5.58	1.79	0.55	9.84

Heat-treatment of coal with hydrogen donating compounds

A coal sample and 9,10-dihydroanthracene (abbreviated as DHA) or 9,10-dihydro-phenanthrene (DHP) were put in a sealed tube (Pyrex, 6 mm inner diameter x 100 mm long) in

the weight ratio of 1:1 (100 mg each), the tube being inserted into the electric furnace preheated at the determined temperature (380 – 420°C), and kept for 5 min. The temperature of the inside of the sealed tube was found to reach the desired temperature within 2 min, the heating rate being about 200 K/min. After 5 min passed, the sealed tube was taken out and the products were recovered by breaking the tube and washing the inside of the tube with dichloromethane. After the addition of an appropriate internal standard, the consumption of DHA or DHP were determined by GC.

Heat-treatment of coal model compounds with hydrogen donating compounds

As the coal model compounds possessing bridge bonds, DPE, BPE, DNE and DBN were employed. Both a model compound and donor (DHA or DHP) were used in 0.25 mmol in the reaction. The reaction and analytical procedures were the same as cited in the previous section.

Solvent extraction of coal and measurement of solution ^{1}H-NMR of the extract

Coal was treated with pyridine and separated into pyridine soluble and pyridine insoluble fractions by Soxhlet extraction. ^{1}H-NMR measurement of pyridine soluble fraction was conducted in pyridine-d_5. 100 mg of extract was put into 1 ml of pyridine-d_5, ^{1}H-NMR spectrum of the solution being measured under the conventional conditions. The heat-treatment of the extract with DHA was conducted at 420°C for 5 min in a sealed tube and recovered products submitted to ^{1}H-NMR measurement. TKS (tetrakis(trimethylsilyl)silane) was added to the solution in determined weight in order to quantify each type of hydrogen. The assignments of type of hydrogen were determined from the reported values in many papers[12], CH_3 at γ-position to aromatic ring or in longer chains (γ^+CH_3, 0.5-1.1 ppm), CH_2 and CH at γ-position to aromatic ring or in longer chains and β-position of aromatic ring (βCH_2,CH, 1.1-2.0 ppm), CH_3 at α-position to aromatic ring (αCH_3, 2.0-2.4 ppm) and CH_2 and CH at α-position to aromatic

ring (αCH_2,CH, 2.4-4.0 ppm).

Diffuse reflectance FT-IR measurement

The coal samples treated with DHA or DHP at 380 and 420°C for 5 min were submitted to the diffuse reflectance FT-IR measurement. The method for this measurement was same as chapter 1: Diffuse reflectance FT-IR spectra were recorded on a Shimadzu FTIR-8100M spectrometer equipped with DRS-8000 unit. The coal sample (30 mg) was mixed with pure KBr (270 mg) by using a mechanical grounder. Scan number of 1024 was applied for each measurement and obtained data were treated with Kubelka-Munk conversion which is conventional method to get quantitative data from diffuse reflectance FT-IR spectra.

2-3. Results and Discussion

2-3-1. The reaction of coal with hydrogen donating compound

The heat-treatment of the 17 sample coals with the hydrogen donating compound, DHA or DHP was carried out at 380 or 420°C for 5 min in a sealed tube. The reaction gave the corresponding dehydrogenated compound, anthracene or phenanthrene, as the major product along with minor amounts of tetrahydro-derivatives (mainly 1,2,3,4-tetrahydro isomer). When either DHA or DHP was treated in a sealed tube without coal (blank runs), there observed negligible amounts of tetrahydro-derivatives. These results suggested that tetrahydro-derivatives were derived from coal-induced disproportionation of DHA or DHP. The amounts of hydrogen transferred from DHA or DHP to coal were evaluated according to the following equation:

The amount of hydrogen transferred (mg-H_2/g-daf coal) = (wt of anthracene or phenanthrene x 2/178 - wt of tetrahydro-derivatives x 2/182) x 1000/wt of daf coal

The results of the reaction of coal with the hydrogen donating compounds were shown in Figure 2-1. The lower the rank of the coals was, the more amounts of hydrogen in hydrogen donor were

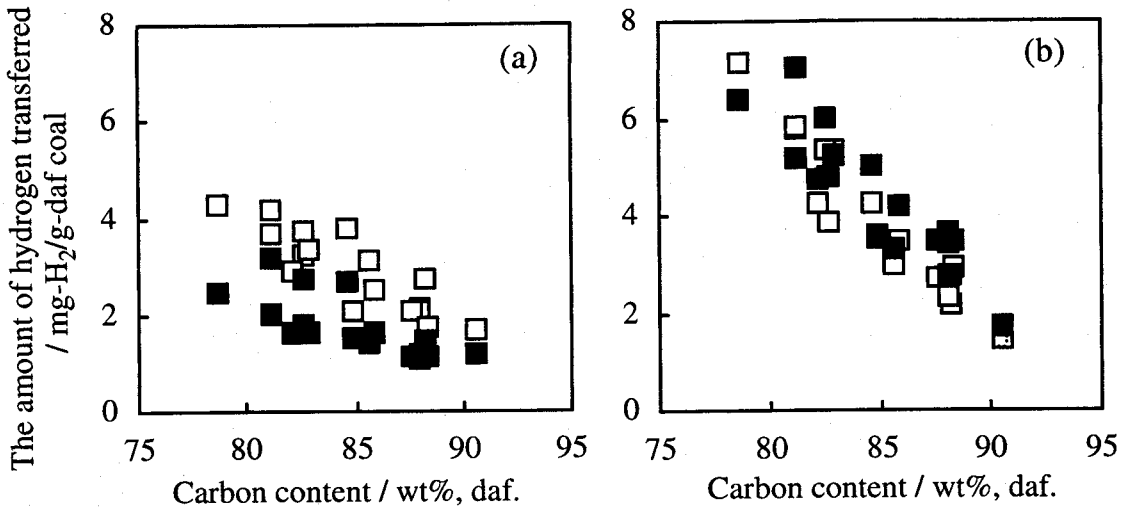

Figure 2-1. The amount of hydrogen transferred during the heat-treatment of coal with DHA(□) or DHP(■) at (a) 380°C and (b) 420°C.

consumed. As it had already been reported, one of the important reactions at around 400°C was considered as the bond cleavage reactions of bridge bonds contained in coal molecule. The results obtained here agreed with the hypothesis that lower rank coals have larger amount of easily cleavable bonds such as dialkyl or aryl-alkyl ether bonds due to their higher contents of oxygen.

It was interesting to note that the amounts of hydrogen transferred from DHP were larger than those from DHA in the reaction at 420°C, while at 380°C, DHA tended to donate more amounts of hydrogen to coal than DHP did. Then, I also tried the heat-treatment of KP and WW coals with hydrogen donating compounds at 400°C. The results were shown in Figure 2-2, these including the results from the heat-treatment at 380 and 420°C. In both coals, there was a crossing point between the amount of hydrogen transferred from DHA to coal and that from DHP to coal at around 400°C. Therefore, the contribution of DHP to the reactions occurred in the heat-treatment of coal with hydrogen donor should be important at high temperature. It might be considered that the bond cleavage reaction in the heat-treatment was dependent on the type of the hydrogen donating compounds. Supposing the occurrence of bond cleavage reaction by the stabilization of generated radicals, I could not explain the present phenomena shown in Figure 2-

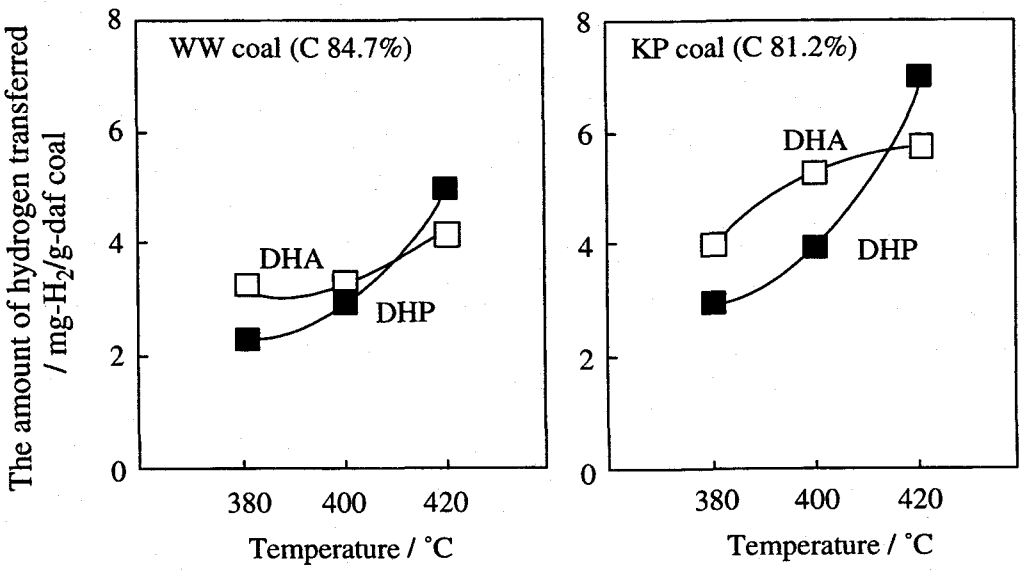

Figure 2-2. The effect of temperature on the amount of hydrogen trasferred on the reaction of coal with DHA (□) or DHP (■).

2 because DHA is better radical scavenger than DHP[13]. Therefore, in order to compare the reactivity of the hydrogen donating compounds, DHA and DHP, I conducted the reaction of the coal model compounds which have bridges between aromatic moieties, such as 1,2-diphenylethane with the hydrogen donating compounds under the similar conditions to the reaction of coal with hydrogen donor.

2-3-2. Bond cleavage of coal model compounds in the presence of hydrogen donor

Generally, coal macromolecule is considered to consist of aromatic cluster and alkyl bridges or side chains including naphthenic portion, being regarded as cross-linking polymers as a whole. In the proposed coal chemical structure models, there observed several bridge structures between two aromatic rings, such as $-CH_2-CH_2-$, $-CH_2-O-$ or $-CH_2-$ and so on. Although the information concerning about such bridge structure connecting aromatic rings was not enough, these were important in the thermochemical reaction of coal. On the basis of these backgrounds, the heat-treatment of coal model compounds possessing bridge structures, DPE, BPE, DNE and DBN, with hydrogen donating compounds was examined. Among these models, DPE and DNE have dimethylene linkage in their structure, so they are expected to be cleaved at $C_{al}-C_{al}$ and $C_{al}-$

C_{ar} bonds (here, C_{al} and C_{ar} indicate aliphatic and aromatic carbon atoms, respectively). The cleavage reaction at C_{al}-C_{al} undergoes homolytically (equation (1)), and the C_{al}-C_{ar} cleavage occurs by hydrogen attack at *ipso* position followed by β-fission (equation (2)). Also in case of BPE, both types of cleavage reaction were expected toward cleavage reactions at C_{al}-O and C_{ar}-O. On the other hand, since DBN has only monomethylene linkage and no C_{al}-C_{al}, only cleavage reaction at *ipso* position to aromatic ring should occur.

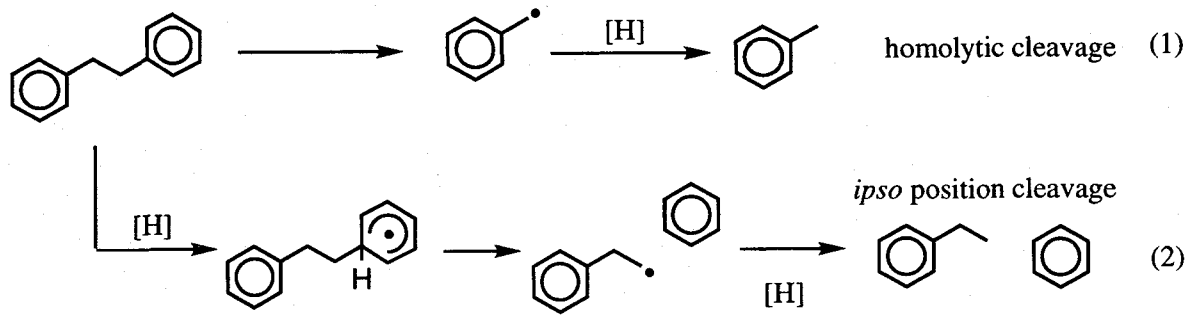

Homolytic cleavage reaction of dimethylene and methylene-ether bonds

The heat-treatment of the model compounds in the presence of DHA or DHP was conducted under the similar conditions to those of coal. The yields of the product obtained from bond cleavage reaction of the model compounds were too high in case of BPE (both phenol and toluene were obtained in more than 95% yield) and too low in case of DPE (toluene, 2 – 4%) and DNE (1-methylnaphthalene, 10 – 12%). In order to discuss the discrepancy in the reactivity of two different hydrogen donating compounds, DHA and DHP, the bridge structure in coal is thought to be cleaved more easily than that in DPE or DNE because the aromatic ring size was relatively large and many substituents attached to aromatic rings in the case of coal. On the other hand, rather high reactivity of BPE with homolytic fission of bridge bond can be easily understood because of small bond dissociation energy of carbon-oxygen. Here, in order to observe much larger difference of the reactivities of DPE and DNE in the presence of either DHA or DHP, the reaction time was prolonged as 60 min. The reaction temperature of BPE was set to 380°C for 5 min because BPE was found to be more reactive than DPE or DNE.

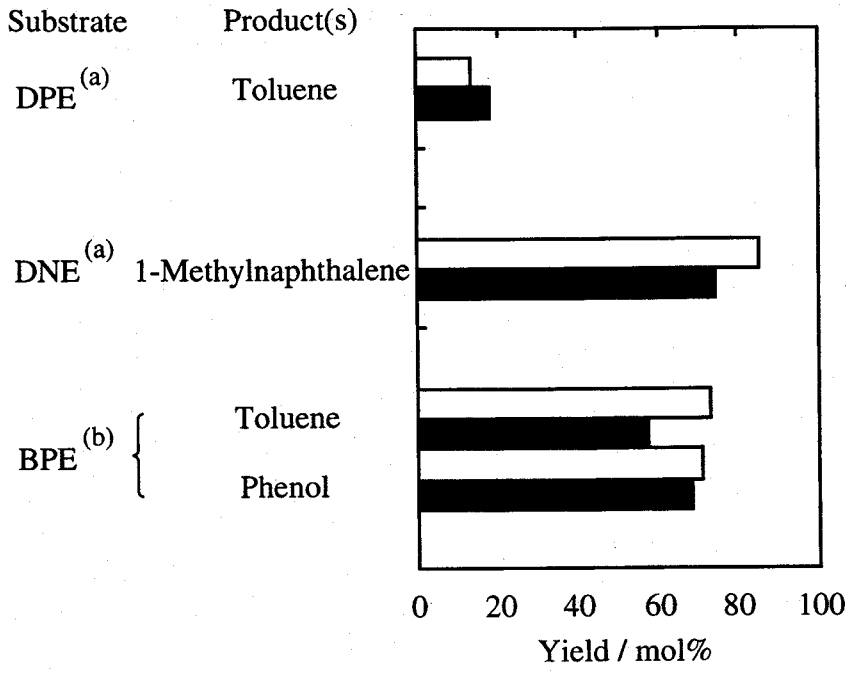

Figure 2-3. The yields of the homolytically bond cleaved products in the reaction of coal model compounds with DHA (□) or DHP (■); (a) 420°C, 60 min, (b) 380°C, 5 min, [Substrate]:[model]=0.25:0.25 (in mmol).

Figure 2-3 shows the yields of the product from homolytic bond cleavage reaction of the model compounds in the presence of two different hydrogen donors. Under the reaction conditions applied here such as at 420°C for 60 min, considerable amounts of DHA or DHP were converted in each blank run so that the yield of anthracene or phenanthrene would not properly reflect the exact amount of DHA or DHP consumed for hydrogen transfer. Therefore, I evaluated the degree of the bond cleavage reaction on the basis of the yields of the cleaved products. The conversion of the model compounds reflects the strength of cleavable bonds (order of bond dissociation energy is $PhCH_2$-OPh << $NapCH_2$-CH_2Nap < $PhCH_2$-CH_2Ph, where Nap and Ph indicate 1-naphthyl and phenyl groups, respectively). DPE showed less reactivity even under these conditions (420°C, 60 min), and slightly higher yield of toluene when DHP was used as the hydrogen donor than in the case of DHA. Actually, the same trend was observed with the reaction of DNE at 420°C, for 5 min. The reason of this experimental result is not clear. It is thought that the less reactivity of DPE might be caused by the small size of aromatic rings and the absence of substituents like -OH or alkyl groups, however, much higher reactivity would be

expected with bridge bonds contained in coal molecule. On the other hand, it should be noted that yields of the homolytic cleavage products from DNE or BPE, 1-methylnaphthalene or toluene and phenol, respectively, were higher when DHA was used as the hydrogen donor than in the case of DHP. These results may come from the fact that DHA has the higher potential to scavenge the radical generated during the heat-treatment[13].

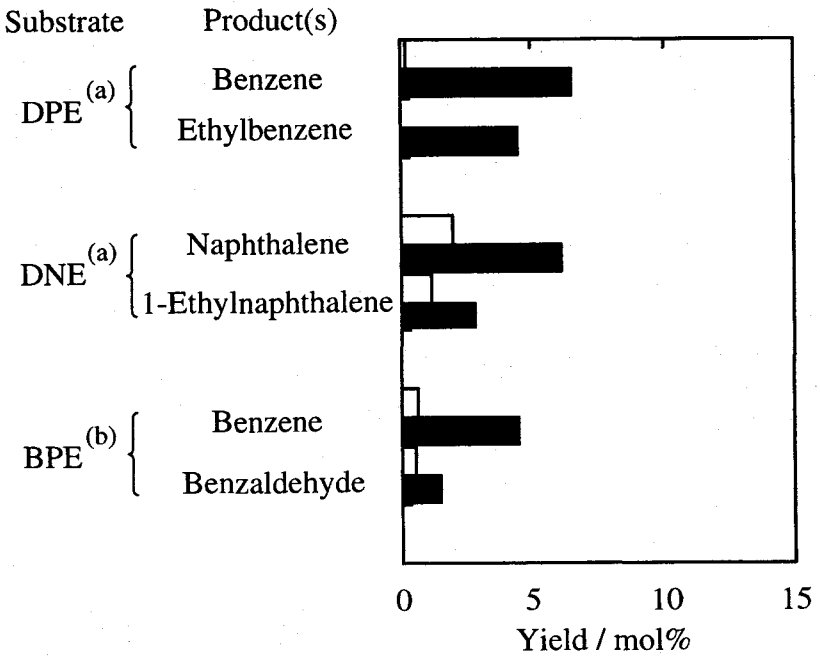

Figure 2-4. The yields of the products from the bond cleavage at *ipso* position in the reaction of coal model compounds with DHA (□) or DHP (■); (a) 420°C, 60 min, (b) 380°C, 5 min, [Substrate]:[model]=0.25:0.25 (in mmol).

Ipso position cleavage reaction of the bridge structure in model compounds

The reaction of DPE or DNE with two different hydrogen donors at 420°C for 60 min, and that of BPE at 380°C for 5 min gave the *ipso* position cleavage products in 0.1 – 6.6% yield (Figure 2-4). These yields from the reaction using DHP were considerably higher than the case of DHA. However, the yields of the products from the cleavage reaction at *ipso* position were relatively low in comparison with those of the homolytic cleavage products. Here, I would like to mention the reports concerning bridge bonds contained in coal[14-17]. RuO_4 catalyzed oxidation reaction has been commonly used for recognition of aliphatic bridge structures and substituent of

coal[14-17] and other fossil fuels[18,19]. This reaction is well known to decompose sp^2 carbons in organic substances selectively. When this reaction was applied to coal, dimethylene bridge connecting two aromatic moieties was confirmed from the formation of succinic acid. However, unfortunately, as for monomethylene bridge this oxidation could not confirm its presence in COM because under these oxidation conditions, the malonic acid is unstable. In generally speaking, the prevailing presence of monomethylene bridge bond in COM is supported by many coal researchers. One support for the presence of monomethylene linkage was shown by Haenel *et al.*[20]. Then, I employed 1,5-dibenzylnaphthalene (DBN) as the possible substrate of coal model compounds. It does not have homolytically cleavable linkages like $-CH_2-CH_2-$ or $-CH_2-O-$, so only the *ipso* position cleavage is expected to take place. Its reaction afforded benzene, toluene, benzylnaphthalene and benzylmethylnaphthalene. However, only small amount of naphthalene derivatives was obtained and the recovery of the substrate was not so high. This could be explained by assuming that some oligomerization or very complicated reaction might occur under the reaction conditions as pointed out in a previous paper[3]. Therefore, I judged the degree of cleavage on the basis of the sum of the yield of benzene and toluene. Also from this result, the *ipso* position cleavage by using DHP could proceed more efficiently than in the case of DHA (Figure 2-5). In this system, strong C_{al}-C_{ar} bond must be cleaved by solvent induced scission. It could be suggested that introduction of hydrogen atom as a result of radical hydrogen transfer or free hydrogen transfer occurred in heat-treatment of coal, and Malhotra *et al.* also mentioned the effectiveness of *ipso* position cleavage

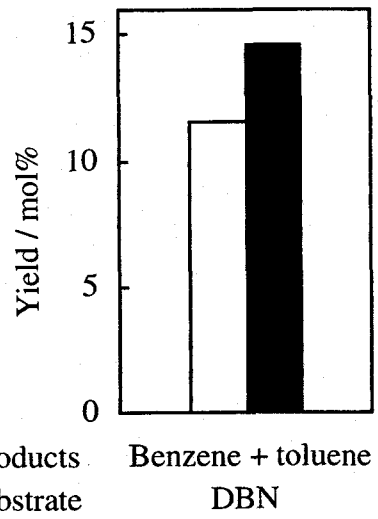

Figure 2-5. The yields of the (bezene+toluene) from the bond cleavage at ipso position in the reaction of DBN with DHA (□) or DHP (■) at 430°C for 60 min [Substrate]:[model]=0.25:0.25 (in mmol).

in liquefaction reaction[21].

Only above discussions could not explain the results shown in Figure 2-1: the larger amount of hydrogen was consumed from DHP than DHA in the reaction of coal with hydrogen donor. I'm considering that the structural feature of coal molecule is important for the explanation. Bond cleavage reactions using models (Figures 2-3 and 2-4) showed that the yields of homolytically cleaved products were higher than those of *ipso* position cleaved products, this being reasonable in terms of their bond energies. Therefore, the hydrogen consumption in the reaction of coal with DHA at 420°C must be higher than that in the presence of DHP, according to the higher hydrogen donatability of DHA. However, the experimental results didn't agree with above expectation: DHP consumed larger amount of hydrogen in the reaction with coal at 420°C. On the other hand, Figure 2-4 showed that *ipso* position cleavage reaction was preferable in the presence of DHP. As the results, I thought that *ipso* position cleavage reaction had a crucial contribution in the reaction of coal with DHP at relatively higher temperature. This strongly indicates that monomethylene linkage is significant bridge bond which governs the coal reactivity.

2-3-3. Bond cleavage reaction occurred in coal

Solvent extraction of coal and ^{1}H-NMR measurements of the extract

In the previous sections, the amount of hydrogen consumed by hydrogen donor compounds was focused in the reaction of coal with hydrogen donor, while the yields of the cleaved products was discussed in the reaction of coal model compounds. Unless the bond cleavage reaction occurs in coal in the presence of hydrogen donor, the results obtained from the reaction of coal with hydrogen donor and that of coal model compounds with hydrogen donor could not be comparable each other. Therefore, I decided to use coal extract instead of coal for the reaction with hydrogen donor compounds. ^{1}H-NMR spectra of pyridine soluble fraction of LS coal and its anthracene treated (420°C, 5 min) fraction were shown in Figure 2-6. In order to

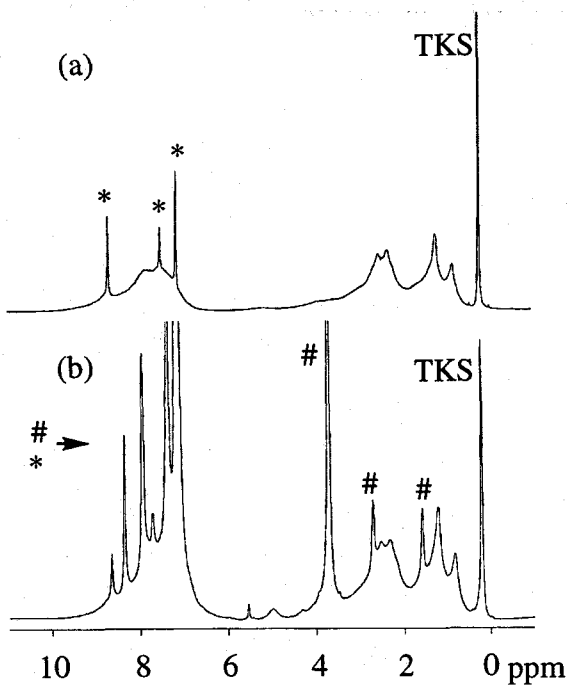

Figure 2-6. ^{1}H-NMR spectra of (a) pyridine soluble fraction and (b) DHA, 420°C treated pyridine soluble fraction of LS coal (C 88.3%). * :signals from pyridine; #: signals from DHA and its derived compounds.

quantify the changes of type of proton, TKS was added as an internal standard. The peak intensities of methyl or methylene protons, the assignments of which were mentioned in an experimental section, were shown in Table 2-2. Each value was based on the peak intensity of TKS. Some of the signals from DHA or THA overlapped to those from coal extracts in the aliphatic region of the spectrum, but the increase of methyl groups was observed clearly after the treatment of coal extract with DHA at 420°C for 5 min. Both homolytic cleavage reaction and *ipso* position cleavage reaction induce the increase of methyl group. Therefore, the results shown in Table 2-2 supported the occurrence of bond cleavage reaction in the reaction of coal extracts with 9,10-dihydro-anthracene. Since coal extract is a part of the coal, the bond cleavage reaction is expected to occur during the heat-treatment of coal with hydrogen donor. On the other hand, the signal intensity of α-methylene in treated coal extract was estimated by subtracting the contribution from DHA and THA from all α-CH_2 regions. The bond cleavage reaction reduced methylene group, however, α-methylene also seemed to increase. This may be caused by the hydrogenation of aromatic ring. Because higher hydrogen donatability of DHA than DHP disagreed with the experimental results from the reaction of coal with hydrogen donor at 420°C for 5 min: more

Table 2-2. Analysis results of ^{1}H-NMR spectra of untreated and DHA treated pyridine soluble fraction of LS coal.

chem. shift (ppm)	assignment	area (TKS=1)	
		untreated	treated
0.5-1.1	γ^+CH_3	0.96	1.19
2.0-2.4	αCH_3	0.56	0.70
2.4-4.0	αCH_2, CH	1.95	2.24

DHP was consumed during the heat-treatment than DHA, so the hydrogenation of aromatic ring is not the main reaction in this heat-treatment.

Diffuse reflectance FT-IR measurements of heat-treated coals

The similar supporting experimental results were obtained from FT-IR measurements of residue of the heat-treatment. Five kinds of coals were treated with DHA or DHP at 420 and 380°C for 5 min, and the reaction residue was recovered by washing the reaction mixture using solvent. In this case, absorption bands of C-H stretching of ArC-H (3040 cm^{-1}), CH_3 (2952 cm^{-1}) and CH_2 (2926 cm^{-1}) were observed and got their peak intensity. Table 2-3 showed the intensity ratios of CH_3 to ArC-H and CH_2 to ArC-H for raw or treated coal samples. Plausible reactions during heat-treatment of coal with hydrogen donor compounds were bond cleavage reaction and hydrogenation of aromatic ring. The former reaction contained *ipso* position cleavage reaction

Table 2-3. FT-IR data of raw and DHP or DHA treated coals.

Sample	Heat-treatment temperature / °C	DHP treated		DHA treated	
		CH_3/ArC-H	CH_2/ArC-H	CH_3/ArC-H	CH_2/ArC-H
KP (C 81.2%)	- [a]	7.9	10.3		
	380	8.4	12.0	8.9	12.7
	420	7.0	9.3	4.9	6.8
WB (C 82.7%)	-	3.6	4.8		
	380	3.4	4.4	3.4	4.8
	420	3.3	4.3	2.9	4.1
WW (C 84.7%)	-	4.4	5.7		
	380	4.3	5.5	4.2	4.9
	420	4.2	5.3	4.2	5.1
PM (C 85.7%)	-	3.3	3.7		
	380	3.5	3.9	nd [b]	nd
	420	3.6	4.2	nd	nd
LS (C 88.3%)	-	2.2	2.3		
	380	2.4	2.7	2.2	2.5
	420	2.3	2.4	2.3	2.6

a) untreated (raw) coal. b) not determined

and homolytic cleavage reaction. The bond cleavage reaction at *ipso* position should correspond to a decrease of ArC-H and an increase of CH_3 according to the change of Ar-CH_2- to Ar-H. Therefore, CH_3/ArC-H is expected to decrease or increase and CH_2/ArC-H should decrease. Homolytic cleavage reaction induces the decrease of CH_2, and decrease of CH_2/ArC-H by the change of -CH_2-CH_2- to 2CH_3. The data shown in Table 2-3 didn't show any clear tendency in comparison of raw coal with treated coals. In case of WB and WW coals, both CH_3/ArC-H and CH_2/ArC-H decreased. These agreed with the structural changes of *ipso* position cleavage reaction. On the other hand, both CH_3/ArC-H and CH_2/ArC-H of PM and LS coals were increased. Since these coals are higher rank among the sample coals applied in this study, they have larger aromatic ring and smaller amounts of bridge bonds. Therefore, the contribution of hydrogenation reaction of aromatic ring may become important. KP coal showed a curious tendency, this might be caused by the removal of solvent soluble fraction: When I washed the reaction mixture by CH_2Cl_2 after the heat-treatment of coal with hydrogen donor, a part of coal was solublized. KP coal had soluble fraction in large amount, 20 wt% in maximum. The structural change in coal was difficult to be detected under these situations.

Above FT-IR results indicated the bond cleavage reaction in coal during heat-treatment. The occurrence of hydrogenation of aromatic ring was also suggested in higher rank coal. Besides, increasing solubility of coal toward CH_2Cl_2 after heat-treatment implied the decomposition of coal molecule, this supporting the bond cleavage reaction to take place in coal.

2-4. References

1 Autrey, T.; Alborn, E. A.; Franz, J. A.; Camaioni, D. M. *Energy Fuels* **1995**, *9*, 420.

2 (a) Futamura, S.; Koyanagi, S.; Kamiya, Y. *Fuel* **1988**, *67*, 436. (b) Futamura, S.; Koyanagi, S.; Kamiya, Y. *Fuel* **1989**, *68*, 130.

3 Murata, S.; Nakamura, M.; Miura, M.; Nomura, M. *Energy Fuels* **1995**, *9*, 849.

4 (a) Korobkov, V. Y.; Grigorieva, E. N.; Bykov, V. I.; Senko, O. V.; Kalechitz, I. V. *Fuel* **1988**, *67*, 657. (b) Korobkov, V. Y.; Grigorieva, E. N.; Bykov, V. I.; Senko, O. V.; Kalechitz, I. V. *Fuel* **1988**, *67*, 663. (c) Korobkov, V. Y.; Grigorieva, E. N.; Bykov, V. I.; Kalechitz, I. V. *Fuel* **1989**, *68*, 262. (d) Korobkov, V. Y.; Grigorieva, E. N.; Bykov, V. I.; Kalechitz, I. V. *Fuel* **1989**, *68*, 1220.

5 Smith, C. M.; Savage, P. E. *Energy Fuels* **1994**, *8*, 545.

6 Murata, S.; Mori, T.; Murakami, A.; Nomura, M. *Energy Fuels* **1995**, *9*, 119.

7 Freund, H.; Matturro, M. G.; Olmstead, W. N.; Reynolds, R. P.; Upton, T. H. *Energy Fuels* **1991**, *5*, 840.

8 McMillen, D. F.; Malhotra, R.; Hum, G. P.; Chang, S.-J. *Energy Fuels* **1987**, *1*, 193.

9 Savage, P. E. *Energy Fuels* **1995**, *9*, 590.

10 Buu-Hoï and Hoán *J. Org. Chem.* **1949**, *14*, 1023.

11 Clar, E.; Lovat, M. M.; Simpaon, M., *Tetrahedron* **1974**, *30*, 3293.

12 For example, Benkhedda, Z.; Landais, P.; Kister, J.; Dereppe, J.-M.; Monthioux, M. *Energy Fuels* **1992**, *6*, 166.

13 Bockrath, J. *J. Am. Chem. Soc.* **1984**, *106*, 135.

14 (a) Stock, L. M.; Tse K.-t., *Fuel* **1983**, *62*, 974. (b) Stock, L. M.; Wang, S.-H. *Fuel* **1985**, *64*, 1713. (c) Stock, L. M.; Wang, S.-H. *Fuel* **1986**, *65*, 1552. (d) Stock, L. M.; Wang, S.-H. *Fuel* **1987**, *66*, 921. (e) Stock, L. M.; Wang, S.-H. *Energy Fuels* **1989**, *3*, 533. (f) Choi, C.-Y.; Wang, S.-H.; Stock, L. M. *Energy Fuels* **1988**, *2*, 37.

15 Blanc, P.; Valisolalao, J.; Albrecht, P.; Kohut, J. P.; Muller, J.F.; Duchene, M *Energy Fuels* **1991**, *5*, 875.

16 Murata, S.; U-esaka, K.; Ino-ue, H.; Nomura, M. *Energy Fuels* **1994**, *8*, 1379.

17 Artok. L.; Murata, S.; Nomura, M.; Satoh T. *Energy Fuels* **1998**, *12*, 391.

18 (a) Mojelsky, T. W.; Igniasiak, T. M.; Frakman, Z.; McIntyre, D. D.; Lown, E. M.; Montgomery, D. S.; Strausz, O. P. *Energy Fuels* **1992**, *6*, 83. (b) Strausz, O. P.; Mojelsky, T.

W.; Lown, E. M. *Fuel* **1992**, *71*, 1355.

19 (a) Boucher, R. J.; Standen, G.; Eglinton, G. *Fuel* **1991**, *70*, 695. (b) Standen, G.; Boucher, R. J.; Eglinton, G.; Hansen, G.; Eglinton, T. I.; Larten, S. R. *Fuel* **1992**, *71*, 31.

20 Haenel, M. W.; Richter, U-B. *Proc. of 9th Int. Conf. Coal Science* **1997**, 223.

21 Malhotra, R.; McMillen, D. F. *Energy Fuels* **1993**, *7*, 227.

Chapter 3. Analysis of Pyrolytic Behavior of Coal by Using Thermogravimetric Analysis

3-1. Introduction

In the early stage of thermoplastic phenomena of coal, pyrolysis of coal molecule is believed to be important. Therefore, many researchers have been investigating coal plasticity in view of pyrolytic behavior of coal. The plastic property of coal was interpreted according to metaplast theory[1-3] where heating of coal generates metaplast which is followed by the generation of semicoke and gas and finally, the semicoke forms coke and gas. Fitzgerald[1], in 1956, proposed a kinetic model of coal carbonization in plastic state. He thought that the carbonization could be explained by the metaplast theory and determined the rate constant for the metaplast generation reaction. This seems to be a great contribution to understanding of plastic properties of coal at an early stage of research of this field. The other theories for the appearance of coal plasticity were the γ-compound theory[4] and the importance of hydrogen transfer[5]. The γ-compound theory refers that the low molecular weight compounds, so called, γ-compounds, occluded in the network structure of coal. They can be extracted in nonpolar solvent particularly chloroform. In this theory, pyrolysis of coal molecule is less important than metaplast theory.

Pyrolytic behavior of coal has been investigating by using various analytical technique such as DSC (differential scanning calorimetry)[6], PMRTA (proton magnetic resonance thermal analysis)[7], high temperature *in situ* ^{1}H-NMR[8], ESR (electron spin resonance)[9] and TGA (thermogravimetric analysis)[2,10-13]. TGA gives us the change of sample weight during heating. This thesis supports metaplast theory by the results in chapters 1 and 2. The previous chapters discussed the transferable hydrogen contained in coal and bond cleavage reaction occurred in coal, these being related to the pyrolysis of coal molecule. In this chapter, TGA of

coal samples were performed in order to investigate pyrolytic behavior of the coals. Then, several parameters regarding coal plasticity derived from TGA data were discussed.

3-2. Experimental

Coal samples

Coal samples applied in this chapter were 18 kinds of coking coals shown in Tables 1-1 and 1-2. The samples were ground to under 100 mesh and dried at 100°C *in vacuo* for more than 6 hours prior to use.

Thermogravimetric analysis (TGA) of coal

A Shimadzu-TGA 50H was used for thermogravimetric analyses of coals. About 10 mg of coal sample was put onto a platinum cell (6 mmϕ x 2.5 mm). Then, the electric furnace was closed and purged with Ar for at least 60 min. The furnace was heated up to 1000°C in the following temperature program: 5 K/min from 100°C to 300°C and 3 K/min from 300°C to 1000°C (standard conditions, other heating rates, 10 K/min and 30 K/min were also applied). Heating rate of 3 K/min was the same rate as that from Gieseler plastometry. Data were collected for every 2 s under standard conditions, data smoothing and making differentiation being conducted on a Shimadzu data processing software. In order to determine the parameters derived from these analyses, I repeated analyses more than three times for each sample to confirm the reproducibility of the data obtained. The errors were estimated to be within 5 % of the value.

TG analysis of coal samples was accompanied by the generation of tar fraction and some of the fraction sticked on bottom surface of inner of the furnace. This fraction was recovered by means of solvent washing and analyzed by field desorption – mass spectroscopy (FD-MS) to observe its molecular weight distribution.

GC analyses of gaseous products evolved during heating by TG apparatus were

conducted by using a Shimadzu GC-8A equipped with a stainless steel column (Porapak Q, 3 m). To accomplish on-line analysis of gaseous products, I used a multiple direction valve on the way from TG furnace to GC inlet. When the furnace heated up to the temperature determined, the valve was switched to introduce 1 mL of gas into GC column. GC analyses were examined at every 50°C from 400°C to 1000°C. Under the applied conditions, H_2, CH_4, C_2H_4, C_2H_6, CO and CO_2 could be detected.

3-3. Results and Discussion

3-3-1. Analyses of parameters obtained from TGA of the sample coals

When coal is heated up under an inert atmosphere, its pyrolysis and devolatilization reactions take place. In this thermogravimetric analysis, coal shows a monotonous weight decreasing, its weight loss being observed as a function of time or temperature. An example of TGA (weight loss) and DTG (rate of weight loss, time differential of TGA) profiles is shown in Figure 3-1. In almost all cases, weight loss started at around 300°C, and DTG curve showed a sharp peak at around 400 to 500°C, which is indicative of the maximum rate of weight loss. Three parameters were defined as shown in Figure 3-1: The temperature at which the maximum rate of weight loss occurs is referred to T_{max}, its maximum rate is R_{max} and the total weight loss when coal was heated up to 1000°C is *WL*.

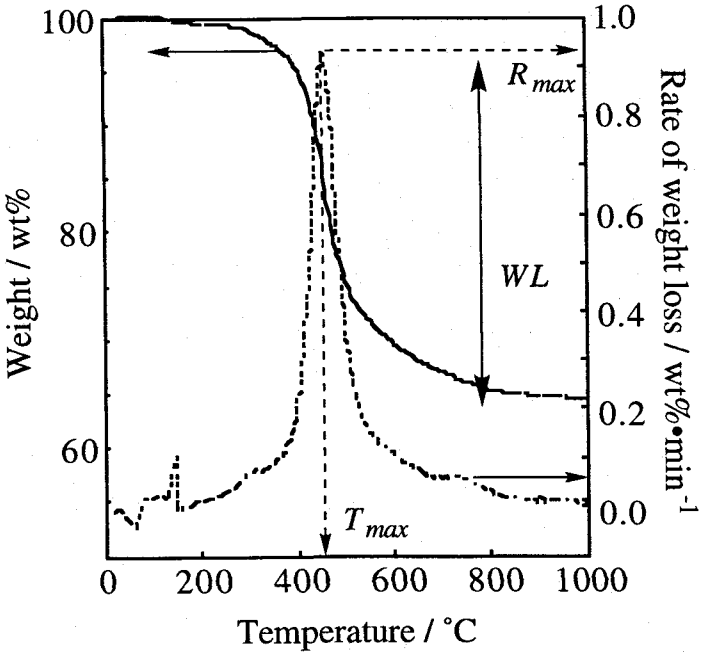

Figure 3-1. Typical TGA and DTG profiles of coal and difinition of the derived parameters such as T_{max}, R_{max} and *WL*.

The temperature at maximum rate of weight loss (T_{max})

The temperature at maximum rate of weight loss, T_{max} determined for 18 sample coals. T_{max} values and the characteristic temperatures of Gieseler plastometry such as softening temperature (ST), maximum fluidity temperature (MFT) and resolidification temperature (RT) for 18 sample coals were plotted as a function of coal rank (Figure 3-2). As an average trend, all these temperatures raised proportionally with increase of carbon content of the coals. This tendency is well known as reported by Solomon *et al.*[13], who conducted TG-FTIR analyses of various coals. However, I found that the T_{max} values were positioned between MFT and RT with only one exception. Though the experimental error including reproducibility for T_{max} was ±5°C, its error does not exert any influence on above tendency against the carbon content of coal and the correlation against the Gieseler temperatures. Therefore, I thought that coal plastic property correlated well to the behavior of weight loss of coal observed by thermogravimetric analysis.

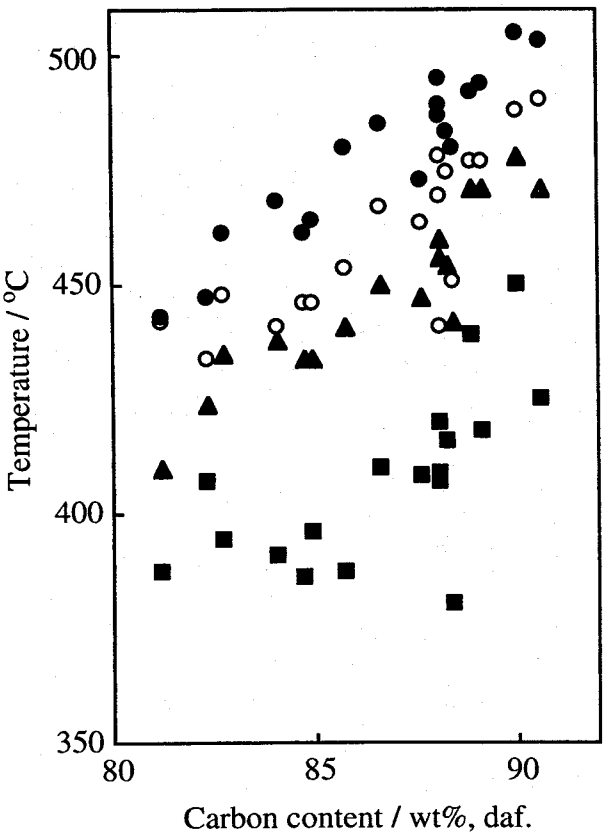

Figure 3-2. The plots of the temperature at the maximum rate of weight loss (T_{max}; ○) and softening (ST; ■), maximum fluidity (MFT; ▲) and resolidification temperature (RT; ●) against carbon content.

The maximum rate of weight loss (R_{max})

Here, I focused on the rate of weight loss which is referred to R_{max}. Figure 3-3 showed the plot of R_{max} against the carbon content of coals. R_{max} showed the following behavior as a function of coal rank: with increasing coal rank, R_{max} value decreased. This is general trend in coal pyrolysis and this parameter was also mentioned by van Krevelen and other

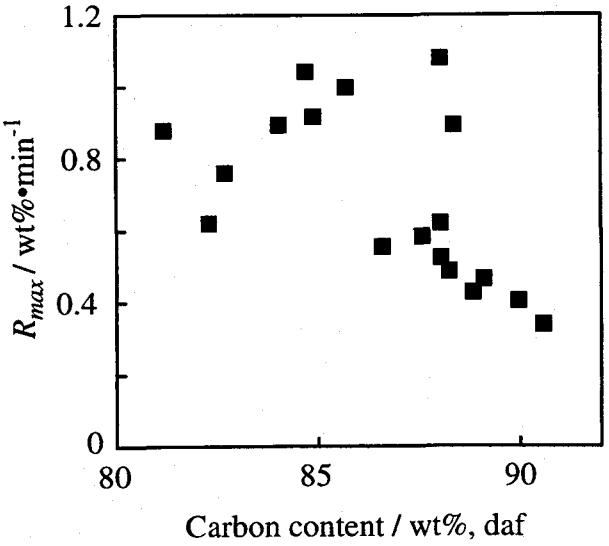

Figure 3-3. The maximum rate of weight loss (R_{max}) for 18 kinds of coal.

researchers[3,11], but the data under the same conditions weren't available. In this study, as shown in Figure 3-3, R_{max} values were scattered. Here, estimated error was enough small (±5 % in maximum) to discuss its tendency. The slight decreasing tendency with increase of coal rank was observed except lower rank coals. The lowest rank coal has high volatility and high aliphaticity, so apparent R_{max} was a higher value while the second lowest rank coal (WB coal) has a less volatility. The one of the reasons of the scattering is due to the different features of chemical components for each coal, for example, WB coal has relatively higher carbon aromaticity evaluated by ^{13}C-NMR measurement, less alkanes were seen in its pyrolysis-GC analysis.

The rank dependence of R_{max} values seemed to be proportional to the whole amount of volatile material. Actually, R_{max} and *WL* had a good correlation as shown in Figure 3-4. Here,

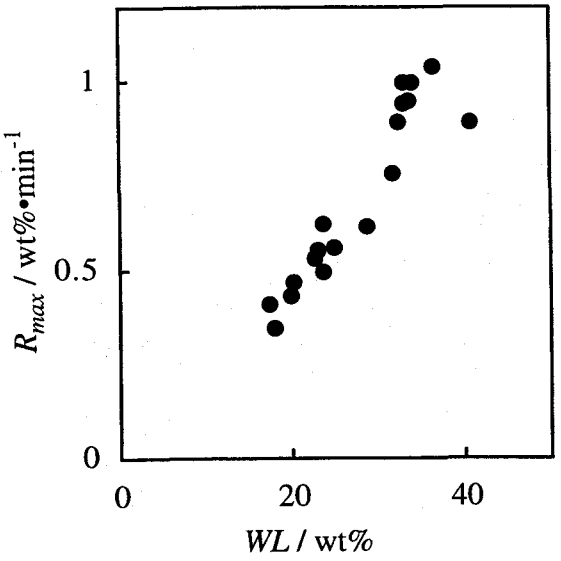

Figure 3-4. Relationship between R_{max} (maximum rate of weight loss) and *WL* (total weight loss up to 1000°C).

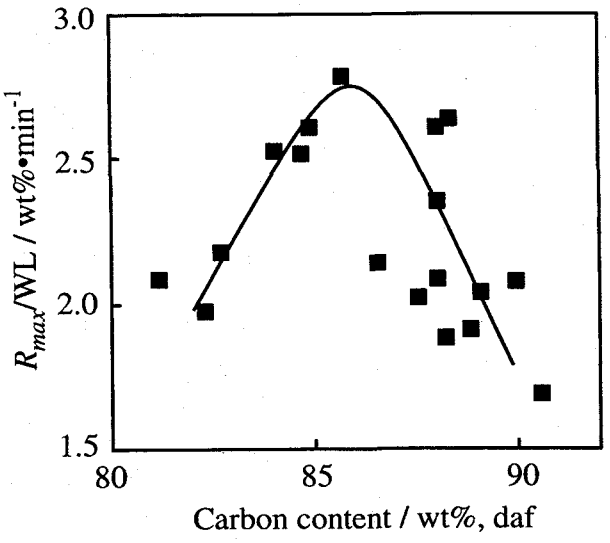

Figure 3-5. R_{max} values normalized by the amount of total weight loss up to 1000°C (*WL*) for 18 kinds of coal.

R_{max}/WL values were calculated by dividing R_{max} value by the amount of total weight loss up to 1000°C (WL) and plotted against carbon content (Figure 3-5). A mountainous curve was obtained, giving a maximum at around carbon content of 85%. If the coal with more amount of volatile material shows the larger R_{max} value, in other words, the correlation in Figure 3-4 was linear completely, the normalized value of R_{max} such as R_{max}/WL should be uniform among all kinds of coal examined. Furthermore, R_{max}/WL value corresponds to evolution rate of the volatile matter fraction, in the whole weight loss, at around T_{max} of each coal. The larger R_{max}/WL means the more effective volatilization is accomplished at T_{max} and *vise versa*. R_{max}/WL values of lower rank coals (80-83 %C) were smaller than those of medium rank coals (85 %C) regardless of the large R_{max} value. These indicated that the lower rank coals evolved volatile materials at wider range of temperature as compared to the others. This is represented by broadened feature of the peak of DTG profile.

Next, I would like to focus on the rank dependence of R_{max}/WL values. Since the maximum R_{max}/WL value at around C 85% can be seen (Figure 3-5), it was noticed that this was very similar to the coal rank dependence of Gieseler maximum fluidity of coal (Figure 1-4). Therefore, I plotted Gieseler maximum fluidity against the R_{max}/WL value. Figure 3-6 showed the relationship between Gieseler maximum fluidity and R_{max}/WL value. It is well known that the medium rank bituminous coal with ~85 %C has good fluid property to form good coke, while either high volatile or low volatile bituminous coal has less fluidity. It was clear from Figure 3-6 that R_{max}/WL showed a good correlation to the empirical

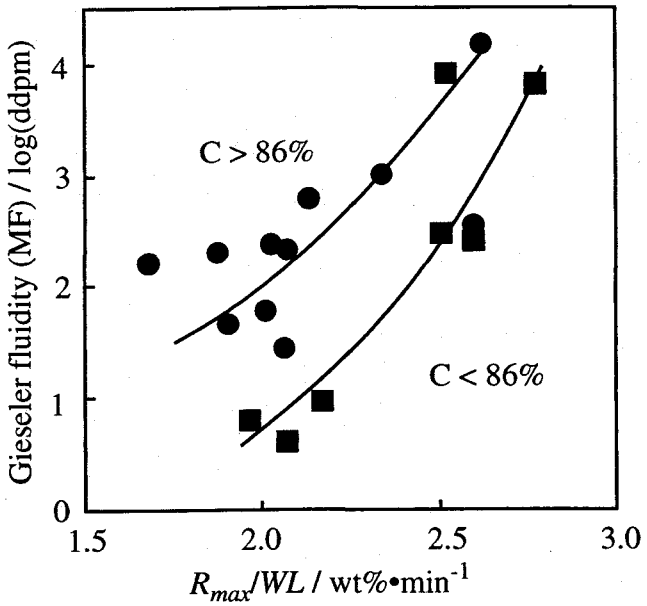

Figure 3-6. The relationship between R_{max}/WL value and Gieseler fluidity of coal.

parameter of plastic property of coal such as Gieseler maximum fluidity. However, it was not the simple correlation and I could not completely explain for some coals with higher fluidity. I suppose this parameter, R_{max}/WL, as a possible another one to show fluidity of coal. The procedure of measurement of Gieseler fluidity of coal is very restricted and sensitive against particle size of coal, packing density or heating rate, and can not be applied to non-coking coal while TGA has potential to be applied for all kinds of coal. In Figure 3-6, I supposed the presence of two correlations depending on the range of carbon content of coal. The higher rank coals (C>86%) showed higher fluidity than the lower rank coal (C<86%) at the same level of R_{max}/WL value. The main portion of the volatile materials observed at around T_{max} was considered to be the tar fraction, which existed in the coal matrix as a part of the low molecular weight lubricant molecules in the state of maximum fluid. This was supported by the experimental results that T_{max} was higher than maximum fluidity temperature. On this assumption, the results shown in Figure 3-6 meant the higher rank coals need smaller amounts of low molecular weight species. This rank dependence might be concerned with the size of lamella sheets comprised of fully condensed or partially saturated aromatic units; the later one stands for hydroaromatic sites. This is based on the following concept: these lamellae play a significant role as the frame of fluid matrix in the metaplast fraction acting as the lubricant and hydroaromatic portions of these lamellae serve to scavenge radicals to avoid fluidity decreasing caused by cross-linking reactions. Although I focused on carbon content of coal when I discussed on the correlation tendency in Figure 3-6, the other factors, for example, maceral composition or type, aromatic ring size or type and density of cross-linking and so on may affect the correlation. Since the pyridine extractabilities of the sample coals might affect the correlation between our parameter and coal plasticity, I conducted pyridine extraction by Soxhlet method and under ultrasonic irradiation at room temperature. However, any clear finding making us discuss the correlation between MF and our proposed parameter could not be obtained.

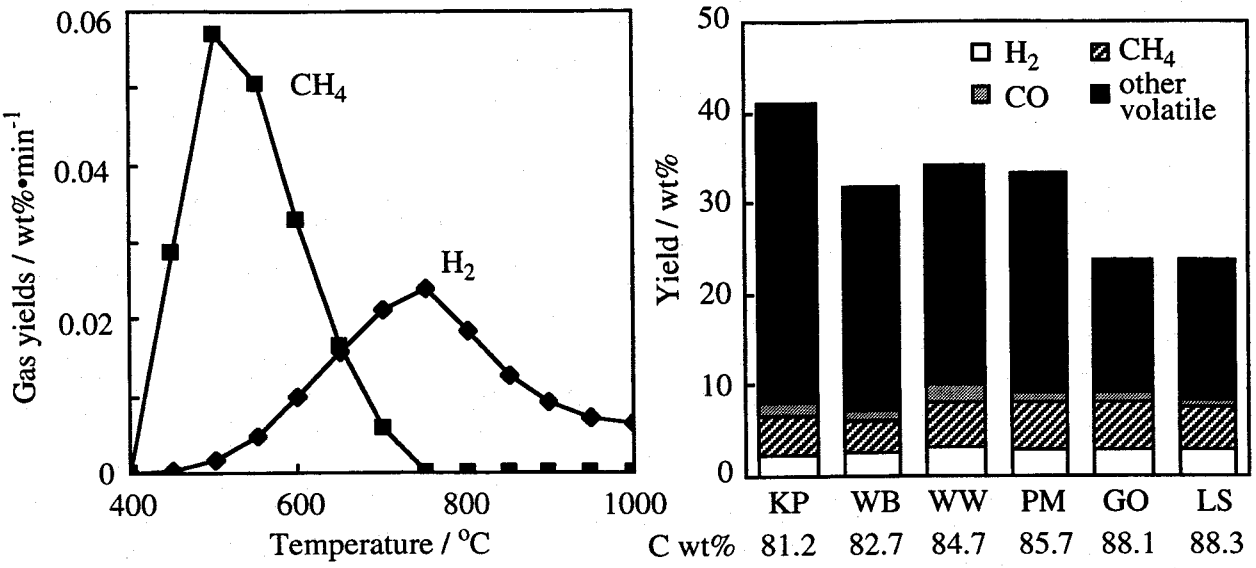

Figure 3-7. Typical figure (WB coal, C 82.7wt%) of gas evolution (left) and H_2, CH_4, and CO yields up to 1000°C relative to the total weight loss (right) of coal.

3-3-2. Analyses of the devolatilized fractions from coal during TGA

TG-GC analysis

In order to evaluate gaseous products generated during TGA, I conducted on-line analysis of evolved gas using six coals, LS, GO, PM, WW, WB and KP coals, whose ultimate and proximate analyses are shown in Tables 1-1 and 1-2, with different carbon content and fluid property. According to the previous study by Solomon *et al.*[13] and other researchers[11,12], CO, CO_2, CH_4 and H_2 are the main gaseous products, while I observed detectable amounts of CH_4, H_2 and CO. CH_4 was generated at the maximum rate around 500°C and H_2 was at 700°C with an example case (WB coal) shown in Figure 3-7. CO was observed only at around 1000°C in detectable amount. The other five coals also showed the similar profile. The temperature at which the rate of evolution of these gases was maximum was not in agreements with the T_{max} of coal. Though the heating rate (3 K/min) was different from Solomon's work (30 K/min)[13], the evolution behavior of CH_4 was consistent with their results, in which CH_4 evolution is correlated to the cross-linking reaction of coal organic portion. The evolution of hydrogen might come from the condensation reaction of aromatics related moieties in coal. As to the total yield of gas shown in Figure 3-7, I could not observe its rank dependence over six coals. In general, VM formation

is larger for the low rank coals than the high rank coals. No rank dependent correlation was found for the formation of each gaseous product. The other gaseous product, CO_2, could not be detected, on the contrary, Solomon *et al.*[13] detected it by using TG-FTIR measurement, where they used a series of Argonne Premium Coal Samples including low rank coal, *e.g.*, North Dakota lignite. They showed the amount of CO_2 depended on coal rank: lower rank coal evolves much more amount of CO_2. For coal samples used in this chapter, the amount of CO_2 evolution is considered to be less relative to that of tar fraction. Even if CO_2 evolution could not be detected due to the lower sensitivity of the apparatus, the range of evolution temperature is not consistent with T_{max} according to Solomon's work, so that assumed that the main portion of weight loss at around T_{max} corresponds to tar fraction. Yield of C_2 gases were also very small, and it was consistent with the analysis of side chains in coal[14], which referred that longer aliphatic side chain than C_2 were small amount relative to methyl substituents.

Analysis of tar fraction

In order to get information about the molecular weight distributions of the tar fraction evolved up to T_{max}, I recovered tarry substance remained at the outlet of the TG furnace. In this experiment, the sample coal was heated up to (T_{max}+ 50)°C because this temperature is considered to be enough high to recover the tar fraction evolved up to around T_{max}. Analysis of coal tar by mass spectrometry is extensively accepted. Some researchers measured the mass spectroscopy of coal tar by field ionization (FI), field desorption (FD) and fast atom bombardment (FAB)[15-17]. FD method for devolatilization and ionization was applied here since this method could observe the components with 3000 Da, while FI and FAB can detect up to 900 Da or so. Figure 3-8 indicates the FD-MS spectra for the tar fraction recovered from heat-treatment of six kinds of coals (LS, GO, PM, WW, WB and KP). The molecular weight range observed was 200 to 1000 Da. According to FD-MS method, it was difficult to detect lower molecular weight materials than 200 Da. However, when analyzed this fraction by GC, some

kinds of compounds, whose retention time correspond to those of anthracene and pyrene, could be detected. This indicated that tar fractions contain various kinds of compounds, aliphatic and aromatic hydrocarbons, molecular weights of which are from less than 200 to 1000 Da. In Figure 3-8, a series of aliphatic components, these being appeared in the same interval (m/z=14), can be seen along with the unidentified components (thought to be aromatic compounds) as the base peaks. For the higher rank coal, relatively low ratio of aliphatic components to aromatic compounds and wider distributions of molecular weights were observed with its tar fraction. Therefore, relatively lower molecules (detected here as 400-800 Da) play an important role in appearance of plastic state. For the components detected by GC, similar rank dependence and relation of aliphatic and other components were observed. Regarding to the lower molecules up to 1000 Da detected by GC and FD-MS, the different rank coals have provided volatile

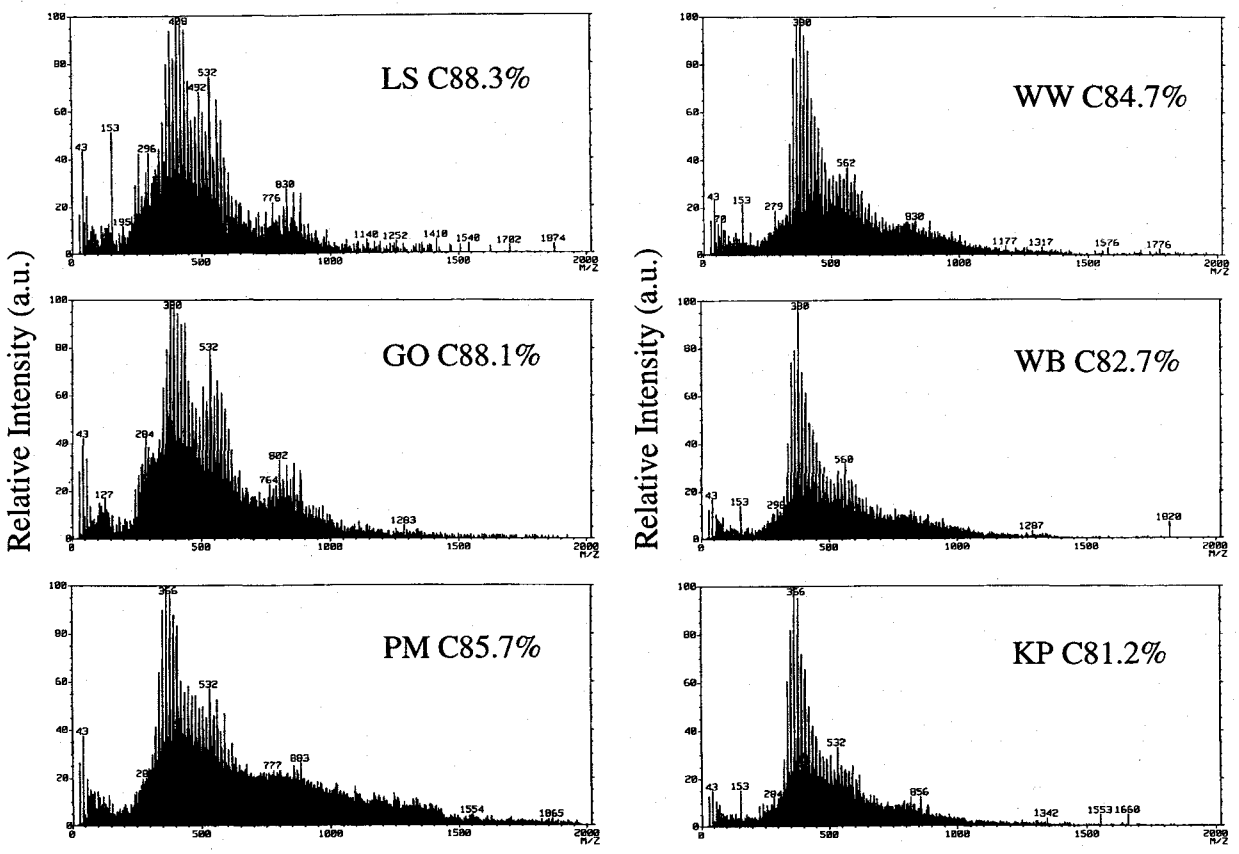

Figure 3-8. Field desorption (FD) mass chromatogram of the tar fractions recovered after the heat treatment up to (T_{max}+50) °C.

components with different composition. These volatile components are considered to act as the lubricant species at their fluid states. Now I can explain Figure 3-6 in terms of both the size of aromatic lamellar moieties and the composition of low molecular weight materials, the correlation in Figure 3-6 indicates lower rank coals (C<86%) have low fluidity compared to higher rank coals (C>86%) at the same level of R_{max}/WL value. This might be explained by the following concepts: (1) Aromatic clusters constituting the frame of fluid matrix is smaller in lower rank coals than in higher rank coals, this causes unfavorable arrangement of matrix for effective fluidity. (2) Aliphatic components are believed not to act as effective lubricant against the fluid matrix. Therefore, in lower rank coals, both small size of aromatic rings and relatively larger ratio of aliphatic components to aromatic compounds in lubricant species lead to less fluidity.

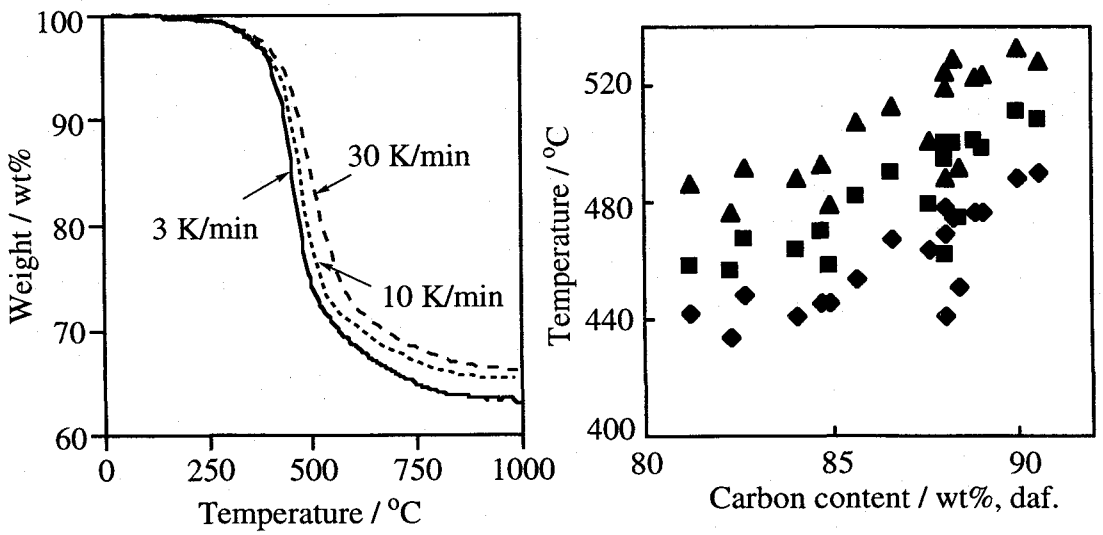

Figure 3-9. The TGA (left) profile of Pittston-MV (PM) coal and T_{max} (right) values of six kinds of coal at heating rate of 3 K/min (◆), 10 K/min (■) and 30 K/min (▲).

3-3-3. Effect of heating rate

The higher heating rate was reported to assist the development of coal plastic properties even with non-caking coal[18,19]. I also performed TG analysis at the different heating rates for 18 kinds of coal. The results are shown in Figure 3-9. I confirmed the shifts of T_{max} to higher

temperature with increasing the heating rate. These behaviors had already been observed previously[3,12]. The proposed parameter, R_{max}/WL, calculated for different heating regimes was correlated with the coal rank, the data being shown in Figure 3-10. Apparently, the higher heating rate led to the larger R_{max}/WL. This seems to agree with the fact that the higher heating rate brings better plastic properties because coal experiences wide range of temperature at the same period during heating. Due to the lack of the data of MF value for the higher heating rate I could not compare MF with R_{max}/WL value. If I could compare the plasticity of coal quantitatively at different heating rates, I would discuss the correlation between the plasticity and the parameter obtained from TGA. The parameter of R_{max}/WL defined as the differential of the

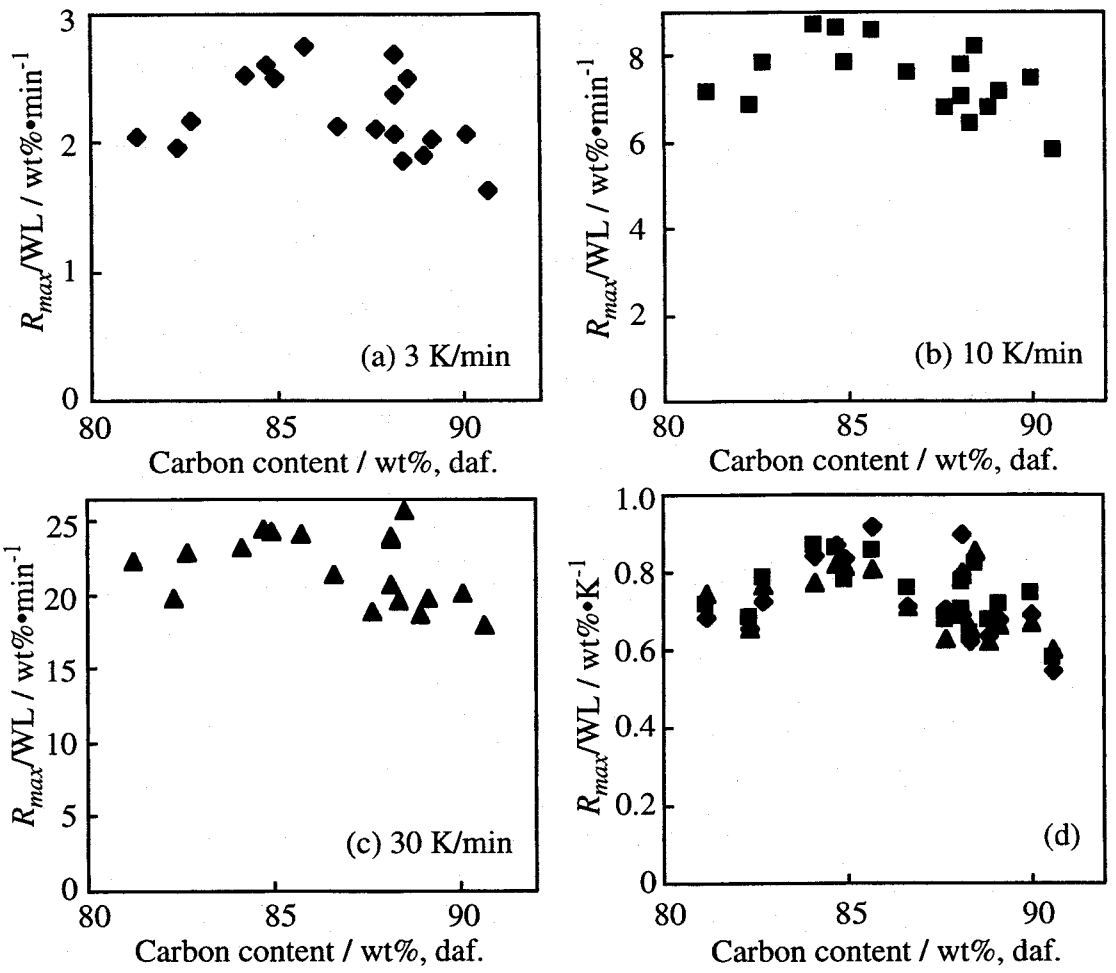

Figure 3-10. R_{max}/WL values at different heating rate, 3 K/min (a, standard conditions, ◆), 10 K/min (b, ■) and 30 K/min (c, ▲), the vertical axis is wt%•min^{-1} for (a) to (c) anc wt%•K^{-1} for (d).

rate of weight loss, based on time. Here, in order to consider this parameter based on temperature and convert its unit from wt%•min^{-1} to wt%•K^{-1}, R_{max}/WL could be divided by the heating rate. These values are shown in Figure 3-10(d), indicating that the same rank dependence can be seen even at higher heating rate. As far as the heating rate up to 30 K/min, the evolution tendency of the volatile or pyrolyzed materials did not change among a series of coal. At higher heating rate, many reactions and physical changes can occur simultaneously, this strongly affecting to the development of plastic properties of coal.

3-4. Reference

1 Fitzgerald, D. *Trans. Farad. Soc.* **1956**, 362.

2 Solomon, P. R.; Best, P. E.; Yu, Z. Z.; Charpenay, S. *Energy Fuels* **1992**, *6*, 143.

3 van Krevelen, *Coal*, Elsevier, Amsterdam, 1993.

4 Ouchi, K.; Itoh, H.; Itoh, S.; Makabe, M. *Fuel* **1989**, *68*, 735.

5 Neavel, R. C. *Coal Science I*, Academic press. London, 1982, Chapter 1.

6 Tromp, P. J. J.; Kaptjein, F.; Moulijn, J. A. *Fuel Process. Technol.* **1997**, *15*, 45.

7 (a) Kamie´nski, B.; Pruski, M.; Gerstein, B. C.; Given, P. H. *Energy Fuels* **1987**, *1*, 45. (b) Lynch, L. J.; Webster, D. S.; Sakurovs, R.; Barton, W. A.; Maher, T. P. *Fuel* **1988**, *67*, 579. (c) Lynch, L. J.; Sakurovs, R.; Wevster, D. S.; Redlich, P. J. *Fuel* **1988**, *67*, 1036. (d) Sakurovs, R.; Lynch, L. J. *Fuel* **1993**, *72*, 743.

8 Maroto-Valer, M. M.; Andresen, J. M.; Snape, C. E. *Energy Fuels* **1997**, *11*, 236.

9 (a) Fowler, T. G.; Bartle, K. D.; Kandiyoti, R.; Snape, C. E. *Carbon* **1989**, *27*, 197. (b) Maroto-Valer, M. M.; Atkinson, C. J.; Willmers, R. R.; Snape, C. E. *Energy Fuels* **1998**, *12*, 833.

10 Whiting, L. F.; Langvardt, P. W. *Anal. Chem.* **1984**, *56*, 1755.

11 Huang, H.; Wang, K.; Klein, M. T.; Calkins, W. H. *ACS Div. Fuel Chem. Prep.* **1995**, *40*,

465.

12 Inaba, A. *ACS Div. Fuel Chem. Prep.* **1996**, *41*, 1187.

13 Charpenay, S.; Serio, M. A.; Bassilakis, R.; Solomon, P. R. *Energy Fuels* **1996**, *10*, 19.

14 Artok, L.; Murata, S.; Nomura, M.; Satoh, T. *Energy Fuels* **1998**, *12*, 391.

15 Marzec, A. *Energy Fuels* **1997**, *11*, 837.

16 Herod, A. A.; Stokes, B. J.; Schulten, H.-R. *Fuel* **1993**, *72*, 31.

17 Marzec, A.; Schulten, H.-R. *Fuel* **1994**, *73*, 1294.

18 Fong, W. S.; Khalil, Y. F.; Peters, W. A.; Howard, J. B. *Fuel* **1986**, *65*, 195.

19 Private communication with Dr. T. Chiba.

Chapter 4. Studies on the Thermoplastic Stage of Coal

4-1. Introduction

Based on the metaplast theory or γ-compound hypothesis, the plastic phenomena of coal was explained. Spiro *et al.*[1] constructed a space-filling model for each coal chemical structure proposed by Given[2], Wiser[3], Solomon[4], and Heredy[5] on the basis of three-dimensional aspects of coal structures and explained the development of plasticity using their coal model concepts. Figure 4-1 shows their schematic illustration of coal pyrolysis. They explained coal pyrolysis as following: The molecules exist in lamellae with flat aromatic planes interrupted by aliphatic protrusions. Thermolysis results

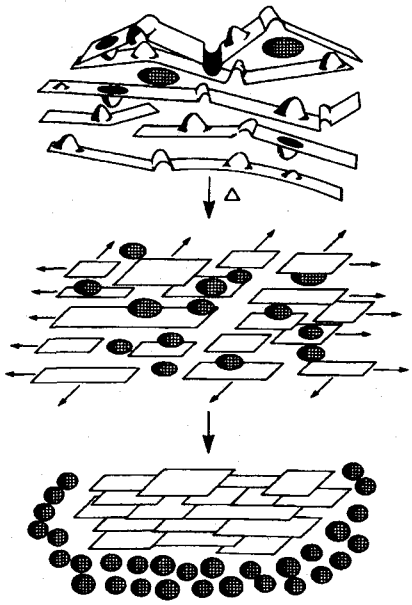

Figure 4-1. Schematic illustration of coal pyrolysis (From Ref. 1a).

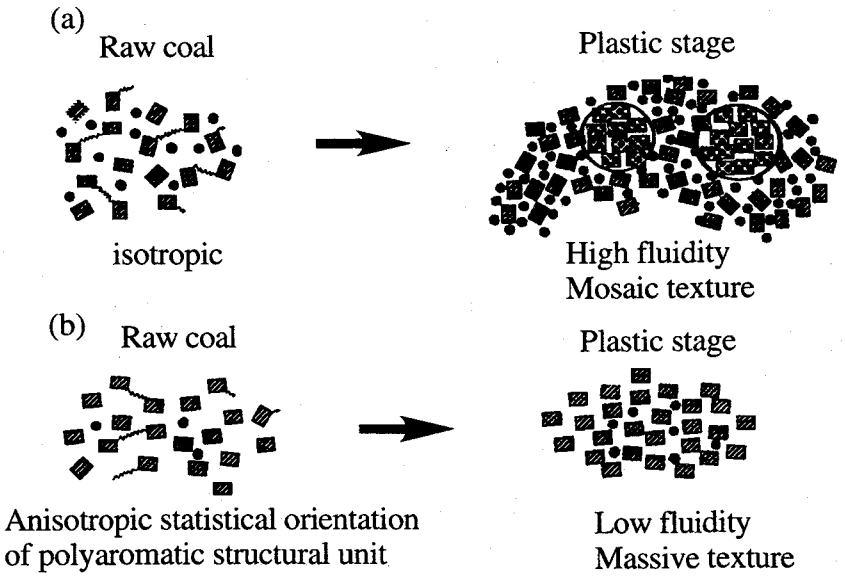

Figure 4-2. Sketches of the two different mechanisms of coke microtexture formation showing (a) first mechanism for medium rank coking coal, and (b) second mechanism for high rank coking coal: □, polyaromatic structural unit; ●, molecular component; ~~~, aliphatic compounds (From Ref. 6b).

in enhanced parallelism of aryl planes accompanied by two-dimensional mobility. When lubricating fragments and gases diffuse from the planes, the char and pore system of the semicoke develops. Fortin *et al.*[6] represented the difference of plasticity with coal rank from the approach by TEM observation of microtexture of coals (Figure 4-2).

In the past two decades, the studies on chemical structure of coal were developed remarkably. Shinn[7] proposed the well-known chemical structure model of US bituminous coal in 1984, the studies on chemical structure for coals being followed by one of Nomura *et al.*[8,9], Hatcher *et al.*[10], Stock *et al.*[11] and Iino *et al.*[12]. Under these situations where coal macromolecular structure was investigated at the level of molecule, I would like to describe coal plasticity and coal structural change during carbonization in terms of the assembly of various kinds of chemical reactions. With referring to the investigations on coal chemical structure, the understanding concerning coal plasticity would be possible. The clarification of plasticity phenomena is believed to lead more effective coal utilization including coke making. I'm interested in chemical structural changes of coal during its heating, hereafter, the thermoplastic stage of coal will be explained based on the results shown in the previous chapters. This chapter also referred the X-ray diffraction and scanning electron microscopic observation of heat-treated coal samples.

4-2. Experimental

Coal samples

Coal samples employed in this chapter were six kinds of coking coals shown in Tables 1-1 and 1-2. The samples were grounded to under 100 mesh and dried at 100°C *in vacuo* for more than 6 hours prior to use. In the measurement of X-ray diffraction, many peaks from inorganic materials contained in coal such as silica appeared sharply, which obstructed the analysis of peaks from coal. Therefore, demineralization was applied to the coal samples before

heat-treatment and XRD measurements according to the following method: 6 g of coal was put into the mixture of 50 ml of HF aq. (36%) and 50 ml of HCl aq. (10%) and stirred at room temperature for 24 h. Coal was separated from acid by filtration of the mixture, and washed repeatedly until filtrate solution doesn't show any acidity. After drying the filtrated sample, demineralized coal was obtained.

Heat-treatment of coal

Heat-treatment of coal was conducted by using a tubular electric furnace, Isuzu DKRO-14K, under nitrogen stream (100 mL/min). Coal was heated up to 300°C at a heating rate of 5 K/min and heated again up to its softening temperature or resolidification temperature (these were determined by Gieseler plastometry, shown in Table 1-2) at a rate of 3 K/min, respectively. After being kept at each temperature for 30 min, each sample was cooled to room temperature slowly (about 2 K/min). Treatment of coal at 1000°C was also conducted by heating up to that temperature at the rate of 30 K/min, then the sample being quenched. The resulting semicoke was grounded roughly, then being submitted to X-ray diffraction measurement.

X-ray diffraction (XRD) measurement

The XRD measurement conditions employed here were as follows: Cu-Kα radiation (λ=1.5405 Å), scan range of angle; 12-50°, scan rate; 10 deg/min. The X-ray apparatus was MAC SCIENCE Co. M18XHF-SRA. The broad peak appeared at around 26° and 43° of 2θ in the diffractograms (Figure 4-3). The peak appeared at lower angle could be divided into two Gaussian peaks assigned as γ-band (~18°) and (002)-band (~26°) by curve fitting method[13]. The crystallite parameters, L_c, d and L_a were defined: L_c means diameter of the aromatic clusters perpendicular to the plane of the sheets, d is layer spacing and L_a indicates the diameter of aromatic sheets. These parameters were calculated as the following equations (1)-(3):

$$L_c = \frac{0.45}{B_{1/2}} \quad (1), \quad d = \frac{\lambda}{2\sin\theta} \quad (2), \quad L_a = \frac{0.92}{B_{1/2}} \quad (3)$$

where, $B_{1/2}$ is full width at half maximum of (002) or (10) band, θ is diffraction angle of the center of the band and λ is Cu-Kα wavelength (1.5405 Å).

4-3. Results and Discussion

4-3-1. XRD observation of heat-treated sample coals

Powder X-ray diffraction (XRD) measurement was conducted for semicoke derived from the sample coals. The crystallite parameters, L_c and d, were obtained on the basis of the diffractogram[13,14], these being shown in Figure 4-4. Each value of raw coal showed clear difference among six kinds of coals with various carbon content such as

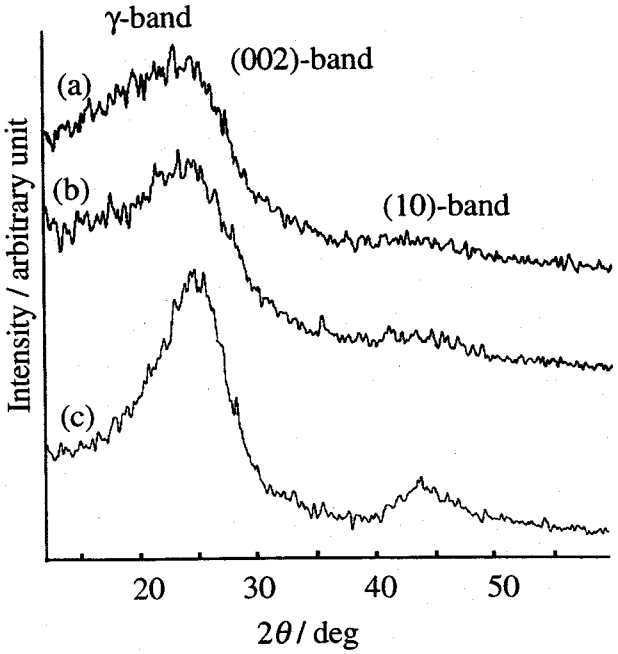

Figure 4-3. Obtained diffractogram of (a) demineralized PM(DPM) coal, (b) DPM coal treated at resolidification temperature (RT, 476°C) and (c) DPM coal treated at 1000°C.

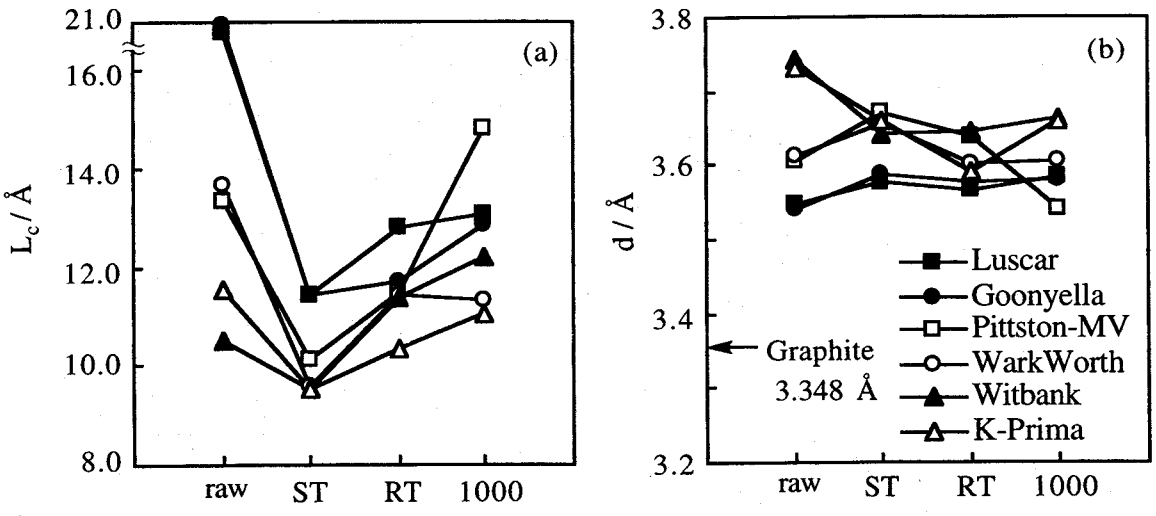

Figure 4-4. XRD parameters of raw and heat treated coal. Heat treated at softening temperature (ST), resolidification temperature (RT) and 1000°C. (a) L_c, average size of aromatic cluster, (b) d, layer spacing.

81.2% for KP and 88.3% for LS. Low rank coals, KP and WB, had small L_c and large d, on the other hand, high rank coals, LS and GO, had large L_c and small d. These results supported that higher rank coal had more developed aromatic cluster than lower rank coal as general considerations of coal structure. For the heat-treated coal samples, the parameter, L_c, at first drops by heat-treatment, then, turning to increase by further heat-treatment. This indicates that, the aromatic sheets are disordered by dealkylation of side chains, or bond cleavage reaction accompanying evolution of hydrogen from naphthenic rings at first stage of the heat-treatment. Further heat-treatment induced the turning to the ordered structure *via* the evolution of small molecular-weight fraction and rearrangement of aromatic sheets followed by going through resolidification to form semicoke. On the other hand, the parameter, d, did not show a clear-cut tendency. The heat-treatment of coal at 1000°C generated firm semicoke. The (10)-band was observed in the X-ray diffractogram of the semicoke treated at 1000°C, therefore, L_a, the diameter of aromatic sheets could be calculated. The L_a values were shown in Table 4-1. 35 Å of L_a corresponded to cata-condensed 15 aromatic rings based on C-C bond length in benzene (1.34 Å). After heat-treatment at 1000°C, stacking of aromatic cluster didn't develop so much, however, size of aromatic ring became very large.

Table 4-1. Average diameter of aromatic sheets (L_a) of the calcined samples at 1000°C by tubelar furnace.

Coal	L_a / Å
Luscar	38.3
Goonyella	39.1
Pittston-MV	40.1
WarkWroth	36.5
Witbank	35.1
K-Prima	35.3

SEM has been commonly used for the observation of treated coal or char particles [15,16]. The residues from rapid pyrolysis and semicoke from heat-treatment of the coals at resolidification temperature and 1000°C observed by using SEM. These images are shown in Figure 4-5. Rapid pyrolysis of the coals was conducted by using a Curie-point pyrolyzer at 764°C with a heating rate of >2500 K/s[17]. Yields of semicoke were 73-86 % for pyrolysis at resolidification temperature, 37-61 % for treatment at 1000°C, and 72-81 % for rapid pyrolysis at 764°C. At resolidification temperature, the size of the particles in semicoke was developed more

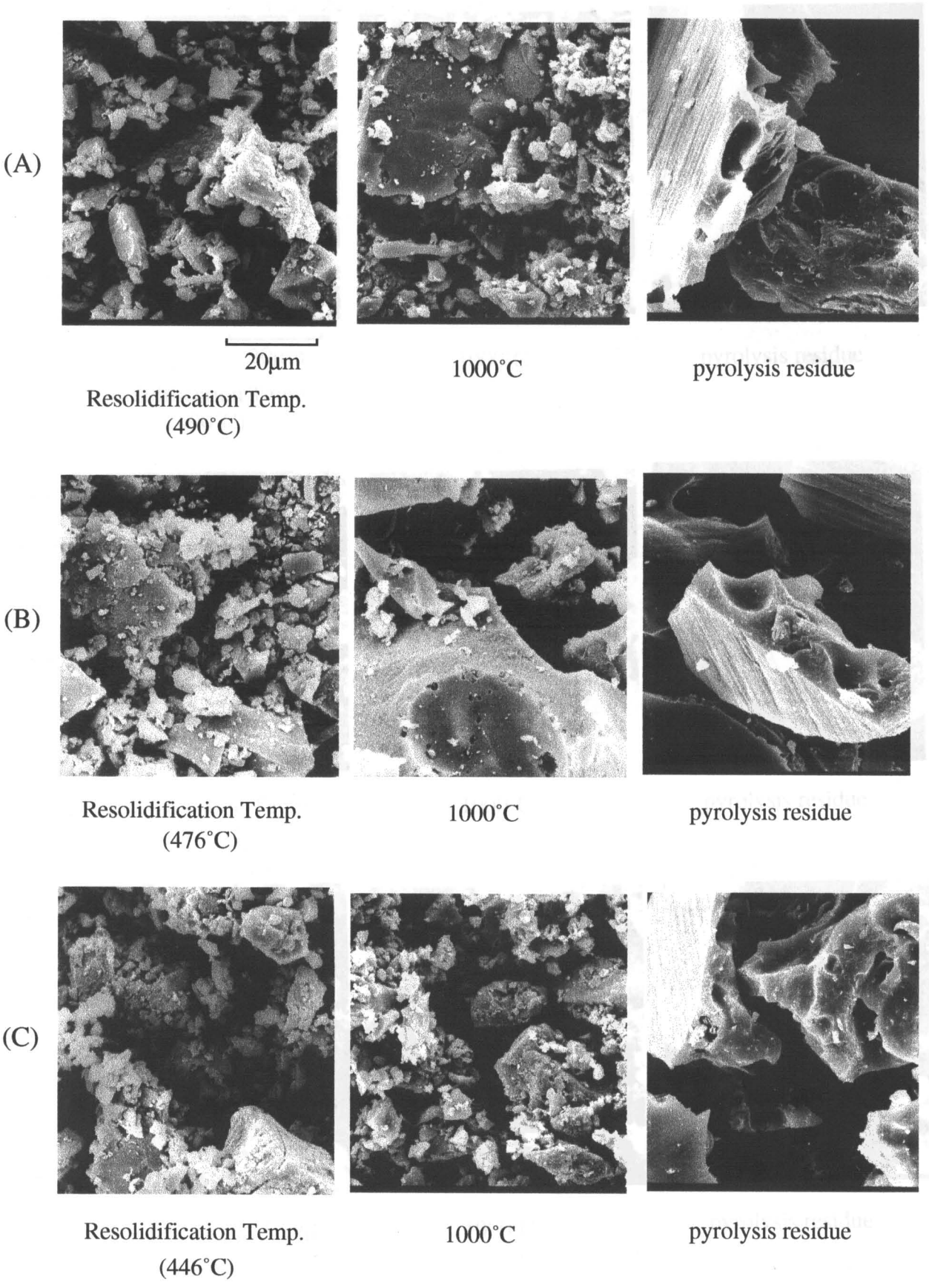

Fgiure 4-5. SEM photographs for the heat-treated (A) Luscar, (B) Pittston-MV and (C) Witbank coals. Heat-treatment was conducted at resolidification temprature and 1000°C by tubelar furnace and at 764°C by Curie-point pyrolyzer.

or less and larger particles could be seen than the case of raw coal. The ordered structure can be seen in the case of PM coal. Furthermore, when the heat-treatment was conducted at 1000°C, the unit of the structure was fairly developed, especially in PM coal. This observation is parallel with the behavior of L_c value from the X-ray diffraction measurement. In all cases, pyrolytic residues showed well ordered structures and well developed pore systems in spite of the higher yields of semicoke, this suggesting that rapid heat-treatment might be effective for coke formation even if low rank coal was used.

4-3-2. Thermoplastic stage of coal

Hereafter, each stage of plastic phenomena will be explained at a molecular level based on the results obtained in this study. Pyrolysis behavior including hydrogen transfer reaction in

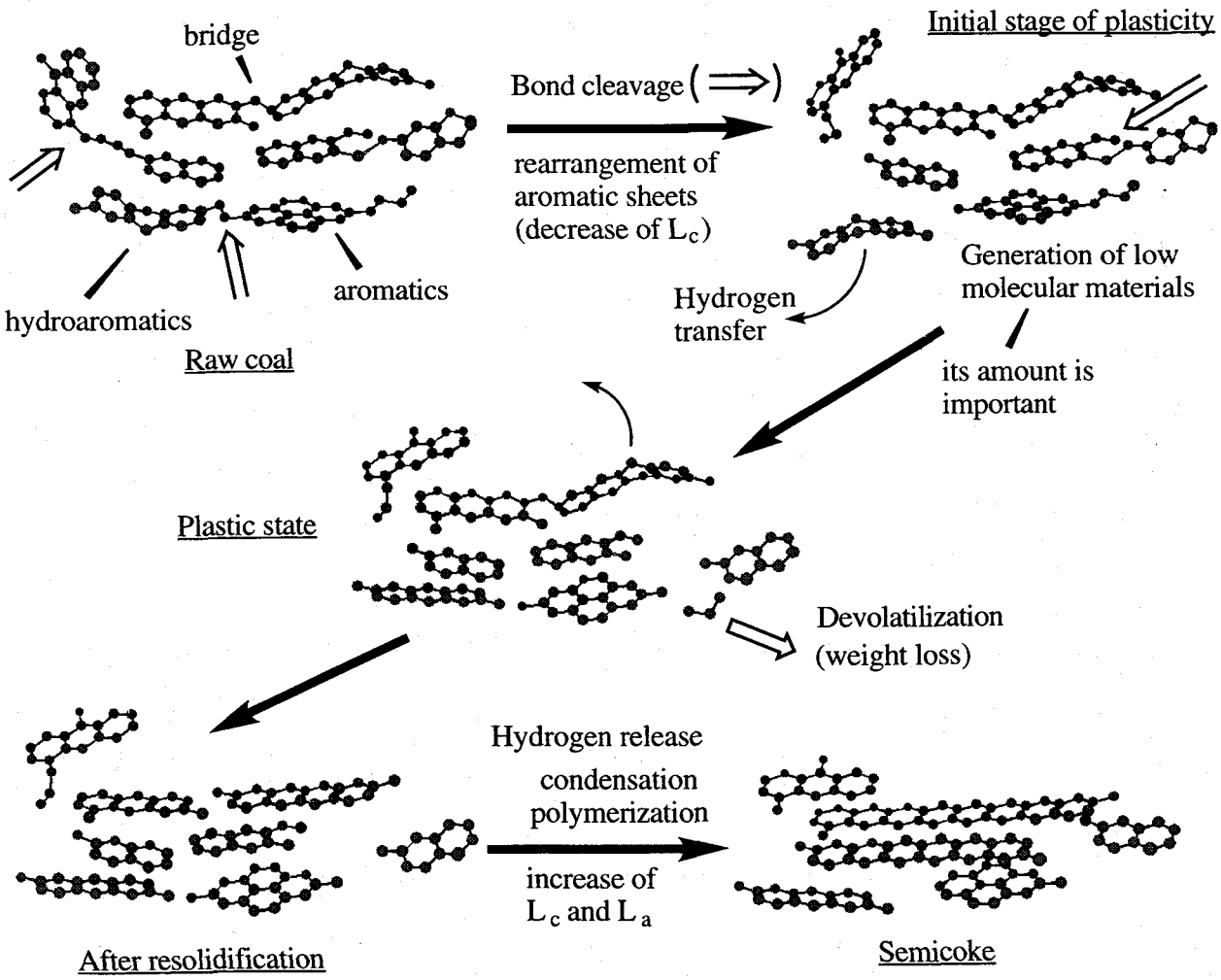

Figure 4-6. Proposed scheme of thermoplastic and carbonization stages.

coal molecule was indicated in view of the explanations of thermoplastic properties of coal. The proposed figure for the concept of coal plasticity was shown in Figure 4-6.

Structural feature of raw coal

First of all, the structural features of raw coal will be mentioned. In general, coal molecule is believed to consist of aromatic rings, bridge bonds connected between aromatic cluster and side chains attached to aromatic rings. Although much effort has been paid to clarify coal structure, the clear-cut understanding is not still available. In this section, I would like to refer the structural features related to the appearance of plastic property of coal. From the analysis of the residue obtained by the reaction of coals with anthracene or naphthacene (chapter 1), existence of hydroaromatic portion was expected as a hydrogen donor site in coal. Presence of hydroaromatic structure wasn't proved directly so far, but it was shown in recent paper[18]: Ruthenium ion catalyzed oxidation reaction of coal was conducted by Artok *et al.* They detected aliphatic polycarboxylic acid from the water soluble fractions of the oxidation products, this indicating the presence of hydroaromatic structure. Based on the results in chapter 2, I proposed that monomethylene linkage is the major bridge bonds connecting between aromatic moieties. Such linkage could be cleaved at *ipso* position to substituted aromatic moieties by the attack of hydrogen provided from hydrogen donor. Concerning with the aromatic portion of coal, the preceding XRD results exhibited the rank dependence of L_c and d value: higher rank coal has larger L_c and smaller d values. Solum *et al.*[19] measured solid state ^{13}C-NMR spectra of the Argonne Premium Coal samples, and evaluated the number of aromatic carbon per cluster. According to their results, the number of aromatic carbon per cluster was 9 for North Dakota lignite and 20 for Pocahontas low volatile bituminous coal. Even recently, Maroto-Valer *et al.*[20] also measured ^{13}C-NMR spectra of coal by more quantitative method. Their results showed the numbers of aromatic carbon per cluster were 15-18 for medium volatile bituminous coals.

Initial stage of plasticity

When heating coal up to around 400°C, coal becomes to have fluidity. In this stage, pyrolysis of coal molecule must be started. In chapter 2, I conducted the reaction of coal or coal model compounds with hydrogen donor compounds. Hydrogen transfer from DHA or DHP to coal occurred even at 380°C. From the reaction of model compounds with hydrogen donor, weaker bonds such as methylene ether bond cleaved preferentially. These results supported the bond cleavage reaction at early stage of coal plasticity, because softening temperatures of coking coal ranged from 380 to 450°C. Generated radicals from the bond cleavage reactions were stabilized by the donatable hydrogen. Therefore, the amount of transferable hydrogen in coal is very important for the appearance of coal plasticity. Lower rank coal needed more amount of transferable hydrogen in order to develop high fluidity relative to higher rank coal did. This could be explained by the population of cleavable bonds in coal: lower rank coal has many cleavable bonds. Based on the metaplast theory, low molecular weight components which contribute to the development of coal plasticity will be generated in this early stage of coal plasticity. Those low molecular weight species should devolatilized during heating. The results in chapter 3 indicated that the amount of low molecular weight species was very important for the appearance of plasticity.

Plastic stage and resolidification

Further heat-treatment induces the state of maximum fluidity followed by the resolidification of coal. In this stage, donatable hydrogen in coal had already consumed to stabilize radicals at the early stage of pyrolysis of coal molecule. Therefore, depolymerization of coal molecule doesn't occur effectively, but polymerization and retrogressive reaction should proceed. Methane formation observed by TG-GC experiments in chapter 3 was occurred remarkably at around resolidification temperature. Methane formation related the cross-linking

reaction of coal molecule as pointed out by Solomon *et al.*[21]. Lost of hydrogen from hydroaromatic site induces the development of aromatic ring system. XRD results showed the increasing of the L_c value when coal was heated at resolidification temperature, this implying the development of aromatic ring system at this temperature range.

To form semicoke after resolidification

After resolidification of coal, weight loss of coal was very small and almost no reaction occurred. However, TG-GC experiments showed the generation of H_2 at high temperature such as 700°C. Such hydrogen loss was considered to come from a condensation reaction of aromatic rings, this reaction leading to the highly development of aromatic ring system. XRD results showed the remarkable development of L_a in the heat-treatment at high temperature. L_a values of heat-treated samples at 1000°C were 35 – 40 Å, these corresponded to 15 aromatic ring system on the average. On the other hand, since L_c value of the same sample wasn't so large. Therefore, aromatic ring size was developed largely whereas the stacking of aromatic sheets didn't become to be large yet in this stage.

4-4. References

1 (a) Spiro, C. L. *Fuel* **1981**, *60*, 1121. (b) Spiro, C. L.; Kosky, P. G. *Fuel* **1982**, *61*, 1080.

2 Given, T. H. *Fuel* **1960**, *39*, 147.

3 Wiser, W. H. *Am. Chem. Soc. Symp. Ser.* **1978**, *71*, 29.

4 Solomon, P. *Am. Chem. Soc.* on New Approaches in Coal Chemistry, Am. Chem. Soc. Regional Meeting, Pittsburgh, Pa, Nov. 1980.

5 Heredy, L. A.; Wender, I. *Am. Chem. Soc. Div. Fuel Chem. Preprints* **1980**, *25*, 38.

6 (a) Fortin, F.; Rouzaud, J. N. *Fuel* **1993**, *72*, 245. (b) Fortin, F.; Rouzaud, J. N. *Fuel* **1994**, *73*, 795.

7 Shinn, J. H. *Fuel* **1984**, *63*, 1187.

8 Nomura, M.; Matsubayashi, K.; Ida, T.; Murata, S. *Fuel Process. Technol.* **1992**, *31*, 169.

9 Supplementary paper (3)

10 Hatcher, P. G.; Faulon, J.-L.; Wenzel, K. A.; Cody, G. D. *Energy Fuels* **1992**, *6*, 813.

11 Stock, L. M.; Muntean, J. V. *Energy Fuels* **1993**, *7*, 704.

12 Nakamura, K.; Takanohashi, T.; Iino, M.; Kumagai, H.; Sato, M.; Yokoyama, S.; Sanada, Y. *Energy Fuels* **1995**, *9*, 1003.

13 (a) Pollack, S. S.; Alexander, L. E. *J. Chem. Eng. Data* **1960**, *5*, 88. (b) Pollack, S. S.; Yen, T. F.; Erdwan, G. J. *Anal. Chem.* **1961**, *33*, 1587.

14 (a) Cuesta, A.; Fernández, M. R.; Pastor, J. M.; Martínez-Alonso, A.; Tascón, J. M. D. *Proc. of 8th ICCS* Oviedo, Spain, 1995, 47. (b) Sousa, J. C.; Torriani, I. L.; Parra, J. B.; Pis, J. J.; Pajares, J. A. *Proc. of 8th ICCS* Oviedo, Spain, 1995, 39.

15 Hurt, R. H.; Davis, K. A.; Yang, N. Y. C.; Headley, T. J.; Mitchell, G. D. *Fuel* **1995**, *74*, 1297.

16 Sugawara, K.; Abe, K.; Sugawara, T.; Nishiyama, Y.; Sholes, M. A. *Fuel* **1995**, *74*, 1823.

17 Nomura, M.; Mori, T.; Murakami, A.; Murata, S.; Nakamura, K. *Energy Fuels* **1995**, *9*, 119.

18 Artok, L.; Murata, S.; Nomura, M.; Satoh, T. *Energy Fuels* **1998**, *12*, 391.

19 Solum, M. S.; Pugmire, R. J.; Grant, D. M. *Energy Fuels* **1989**, *3*, 187.

20 Maroto-Valer, M. M.; Atkinson, C. J.; Willmers, R. R.; Snape, C. E. *Energy Fuels* **1998**, *12*, 833.

21 Solomon, P. R.; Best, P. E.; Yu, Z. Z.; Charpenay, S. *Energy Fuels* **1992**, *6*, 143.

Conclusions

This thesis deals with the analysis of plastic behavior of coal from the viewpoints of reactivity and structural changes of it. The results obtained through this work are summarized as follows:

In chapter 1, the evaluation of donatable hydrogen in coal was investigated. The reactions of coal with four kinds of hydrogen acceptable hydrocarbons (polycyclic aromatic hydrocarbon, PAH) were conducted, and the amount of hydrogen transferred was changed extensively depending on the kind of PAH used. I had found out that the amounts of donatable hydrogen evaluated from the reaction of coal with anthracene correlated with Gieseler fluidity. Therefore, only specific hydrogen atoms having certain reactivity should be effective in the development of plasticity. Concerning the source of donatable hydrogen in coal, the residue after the reaction of coal with PAH was analyzed by solid state ^{13}C-NMR and diffuse reflectance FT-IR spectroscopy. Both results suggested the presence of hydroaromatic structure in coal. This was supported by the reaction of model compounds having hydroaromatic portion or other types of bridge methylene carbons with PAHs.

In chapter 2, the hydrogen transfer reaction in coal was discussed. The reaction of coal or coal model compounds having bridge bonds with hydrogen donor such as 9,10-dihydroanthracene or 9,10-dihydrophenanthrene was conducted. In the reaction of coal with donor, DHP donated larger amount of hydrogen at 420°C than DHA. From the results of heat-treatment of coal model compounds with donor, it was clear that DHP induced *ipso* position cleavage preferentially. Since I could confirm that the bond cleavage reaction occurred in the heat-treatment of coal with donor by ^{1}H-NMR analysis of solvent soluble fraction, the reaction of coal with DHP at 420°C was thought to favor *ipso* position cleavage. Therefore, I proposed that monomethylene linkage is important in coal structure.

In chapter 3, I investigated the plastic properties of 18 kinds of coals by using TG

analysis. It was revealed that the temperatures at the maximum rate of weight loss (T_{max}) positioned between the maximum fluidity temperature and the resolidification temperature determined by Gieseler plastometry. The value of R_{max}/WL, which is normalized rate of weight loss (R_{max}) against the total amount of weight loss (WL) to be well correlated to Gieseler maximum fluidity of coal, was a possible another parameter to show fluidity of coal. The R_{max}/WL value is considered to mean the effectiveness of volatilization at T_{max}. The correlation between R_{max}/WL and MF (Gieseler maximum fluidity of coal) value can be divided into two groups, C<86% and C>86%. In the case of coals having carbon content more than 86%, smaller amounts of volatile materials formed at same level of MF value than the case of C<86%. The volatile materials are existed in coal matrix in fluid state and expected to act as the lubricant species against aromatic sheets. A certain amount of such species was needed to the appearance of plasticity. By the analysis of tar fraction evolved at around T_{max} with FD-MS, we obtained the molecular weight distribution of the resulting tar which showed that higher rank coal had the wider distribution and less aliphatic portion. The effects of heating rate on coal plasticity were also discussed.

Chapter 4 summarized the information about coal plasticity and explained each stage of coal plastic phenomena. The other information about the stacking of aromatic moieties was obtained from X-ray diffraction (XRD) measurements of heat-treated coal samples. XRD gives us the parameters related to the stacking of aromatic moieties, L_c, d and L_a. The minimum L_c values were observed in the heat-treated coal samples at softening temperature, these indicating the disorder of aromatic sheets in the early stage of coal plasticity. The semicoke obtained by the heat-treatment at 1000°C showed 35 – 40 Å of L_a, this indicating the development of aromatic ring.

As indicated above, I analyzed coking coal in the viewpoint of reactivity and structure of coal, and explained the stage of coal plastic phenomena.

Acknowledgement

The work of this thesis has been carried out under the guidance of Professor Masakatsu Nomura of the Department of Molecular Chemistry, Graduate School of Engineering, Osaka University.

The author would like to express his grateful acknowledgement to Professor Masakatsu Nomura for his continuous guidance and encouragement throughout his work.

The author is also indebted to Professor Isao Ikeda and Professor Akio Baba for valuable comments and suggestions.

The author desires to express his sincere thanks to Associate Professors Masahiro Miura and Satoru Murata (present affiliation is Associate Professor of the Advanced Research Projects, Osaka University) for the assistance in the preparation of the manuscripts and many useful suggestions for performing experiments.

The author is much obliged to Professor Mikio Miyake of Japan Advanced Institute of Science and Technology, Hokuriku, Dr. Yoshiharu Yoneyama of Toyama University, Dr. Levent Artok, Dr. Tetsuya Satoh, Dr. Shin-ichi Nakagawa, Mr. Hong Gao and Mr. Tsukasa Chikada for their useful discussion and helpful suggestions during the course of this work.

The author wishes to thank his co-workers, Mr. Akira Yamamoto and Mr. Nobuo Bandoh for their helpful collaboration in the course of the experiments. Many thanks are given to all the other members of the research group of the Nomura Laboratory for their kind help, occasional discussion and friendships.

The author is grateful to Ms. Yoko Miyaji, Ms. Toshiko Muneishi, Mr. Hiromitsu Miyamoto and Mr. Hiroshi Moriguchi at the Analytical Center, Faculty of Engineering, Osaka University for their valuable advice and assistance.

Furthermore, the author thanks JSPS Research Fellowships for Young Scientists for financial support.

Finally, the author particularly intends to appreciate to his mother and brothers for their sympathetic supports.